The Innovation

Review

Surface Enhanced Raman Scattering Revealed by Interfacial Charge-Transfer Transitions

Shan Cong,[1] Xiaohong Liu,[2] Yuxiao Jiang,[1] Wei Zhang,[2,*] and Zhigang Zhao[1,*]

[1]Key Lab of Nanodevices and Applications, Suzhou Institute of Nano-Tech and Nano-Bionics, Chinese Academy of Sciences (CAS), Suzhou 215123, China

[2]Chongqing Institute of Green and Intelligent Technology, Chinese Academy of Sciences, Chongqing 400714, China

*Correspondence: zhangwei@cigit.ac.cn (W.Z.); zgzhao2011@sinano.ac.cn (Z.Z.)

Received: July 9, 2020; Accepted: October 9, 2020; Published: November 25, 2020; https://doi.org/10.1016/j.xinn.2020.100051

GRAPHICAL ABSTRACT

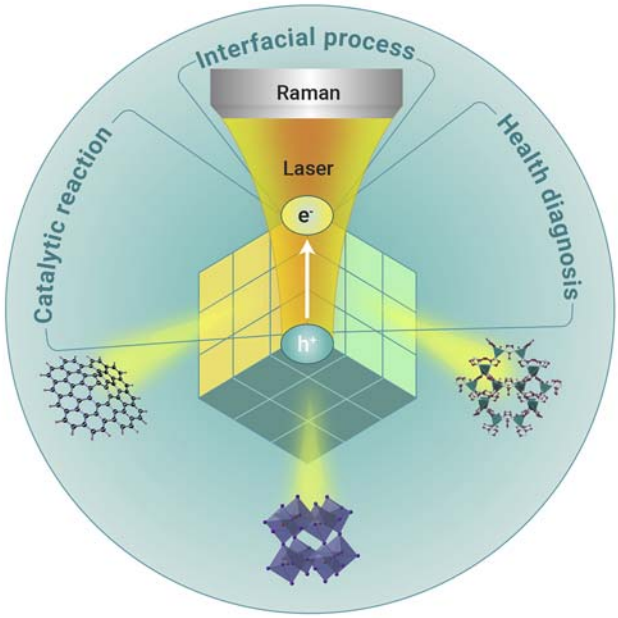

PUBLIC SUMMARY

- Surface-enhanced Raman scattering (SERS) is a fingerprint spectral technique highly dependent on the substrate materials.
- Charge transfer transitions are commonly the major contributors to the boosted SERS activities in non-metal substrates.
- Novel manipulation strategies and extended applications of the versatile substrates are illustrated on the basis of interfacial charge transfer.

CORRESPONDENCE

zhangwei@cigit.ac.cn (W.Z.);
zgzhao2011@sinano.ac.cn (Z.Z.)

https://doi.org/10.1016/j.xinn.2020.100051

Received: July 9, 2020
Accepted: October 9, 2020
Published: November 25, 2020

www.cell.com/the-innovation

Review

Surface Enhanced Raman Scattering Revealed by Interfacial Charge-Transfer Transitions

Shan Cong,[1] Xiaohong Liu,[2] Yuxiao Jiang,[1] Wei Zhang,[2,*] and Zhigang Zhao[1,*]

[1]Key Lab of Nanodevices and Applications, Suzhou Institute of Nano-Tech and Nano-Bionics, Chinese Academy of Sciences (CAS), Suzhou 215123, China

[2]Chongqing Institute of Green and Intelligent Technology, Chinese Academy of Sciences, Chongqing 400714, China

*Correspondence: zhangwei@cigit.ac.cn (W.Z.); zgzhao2011@sinano.ac.cn (Z.Z.)

Received: July 9, 2020; Accepted: October 9, 2020; Published: November 25, 2020; https://doi.org/10.1016/j.xinn.2020.100051

Surface enhanced Raman scattering (SERS) is a fingerprint spectral technique whose performance is highly dependent on the physicochemical properties of the substrate materials. In addition to the traditional plasmonic metal substrates that feature prominent electromagnetic enhancements, boosted SERS activities have been reported recently for various categories of non-metal materials, including graphene, MXenes, transition-metal chalcogens/oxides, and conjugated organic molecules. Although the structural compositions of these semiconducting substrates vary, chemical enhancements induced by interfacial charge transfer are often the major contributors to the overall SERS behavior, which is distinct from that of the traditional SERS based on plasmonic metals. Regarding charge-transfer-induced SERS enhancements, this short review introduces the basic concepts underlying the SERS enhancements, the most recent semiconducting substrates that use novel manipulation strategies, and the extended applications of these versatile substrates.

KEYWORDS: SERS; CHARGE TRANSFER; SEMICONDUCTOR; CHEMICAL MECHANISM; DEFECT ENGINEERING

Introduction

Surface enhanced Raman scattering (SERS) is recognized as a sensitive analysis technique that features molecular structural fingerprints and significantly magnified Raman signals capable of even single-molecule detection. The SERS effects originate from inelastic light scattering by molecules, which is enhanced in the presence of a substrate material, thereby providing active surfaces for both light-matter interaction and molecular adherence. Plasmonic metals such as Au and Ag with corrugated surfaces are the most widely adopted substrate materials, due to their associated field enhancement in the vicinity of the electromagnetic "hot-spot" structure, which usually leads to significant SERS enhancement. In addition to the electromagnetic enhancement in SERS, the changes in molecular polarizability caused by charge-transfer (CT) transitions between the molecules and substrate also play an essential role and are particularly responsible for variations in the spectral shape. More importantly, based on the CT-induced SERS enhancement, numerous types of semiconducting materials, from inorganic to organic, have been developed as novel non-metal SERS substrates with boosted SERS sensitivities comparable even with those of plasmonic metals. Combined with the abundant chemical configurations and optoelectronic functionalities of the semiconducting materials, promising applications have been introduced as being suitable for the SERS technique (Figure 1).

This short review begins with a description of the basic concepts of SERS, which are well established based on the use of traditional metal substrates, and introduces SERS enhancements associated with electromagnetic and chemical contributions. Then, guided by CT-induced chemical enhancement, recently developed representative achievements in the SERS field are discussed, especially those based on the emerging semiconducting substrates, including CT-based SERS active materials, modulation of the CT for improved SERS performance, and applications of SERS in interfacial CT processes. Lastly, the current issues and future developments of SERS are outlined with reference to these semiconducting materials.

Enhanced Raman Scattering Based on Innovations in Substrate Materials

In 1974, the first enhanced Raman spectrum was experimentally observed in pyridine adsorbed onto a roughened Ag electrode,[1] which was then correctly interpreted in 1977 to be an enhancement in the efficiency of Raman scattering itself on the surface of substrates.[2] Since then, materials that serve as substrates for the efficient enhancement of Raman signals have become central to SERS development, from both the theoretical and practical research perspectives. Coinage metals (e.g., Au, Ag, and Cu) with rough surfaces, colloid aggregations, or nanostructures are the most widely considered as candidate SERS substrates. Based on the extensive decades-long study of metal-based SERS, the origin of signal enhancement in the Raman spectrum has been roughly ascribed to two types of contributions, those based on an electromagnetic mechanism (EM) and those based on a chemical mechanism (CM). Although the exact enhancement mechanism remains an open question, great effort has been devoted to clarify the origin of the enhancement and identify new types of semiconducting materials that demonstrate SERS activity, including graphene and its analogs, transition-metal oxides, and conjugated molecules, to name a few. Graphene and its analogs, for instance, have an atomic-scale flat surface that serves as an ideal platform for investigating the CM-induced SERS effect. Metal oxides with varied compositions also serve to boost SERS activities by means of a defect engineering strategy. Conjugated organic compounds and their complexes serving as SERS substrates exhibit almost infinite tunability in their structures. Featuring a prominent CT-induced SERS enhancement, these semiconducting substrates have inherent merits distinct from their metal counterparts, which have enabled a deeper understanding of the SERS mechanism and the broadened application of the SERS technique.

Establishment of Basic Enhancement Mechanism. Since its discovery, the mechanisms responsible for the SERS effect have always been a matter of debate. As noted above, coinage metals such as Ag, Au, and Cu are commonly used as SERS substrates due to their optical absorptions in the visible region. Among these metals, Ag and Au are highly preferred for SERS studies due to their strong plasmonic effect, relative chemical inertness, and well-controlled nanostructures. Based on a platform of Ag and Au substrates, the basic diagram of the SERS enhancement has been established and roughly ascribed to their electromagnetic and chemical contributions.

Electromagnetic Mechanism. As a long-range effect, electromagnetic enhancement is mainly due to a collective of oscillating electron waves on the substrate, typically observed with substrates rich in free electrons that can generate localized surface plasmon resonance (LSPR) upon excitation. The location of the plasmon resonance (ω_p) is a function of the free carrier density (N) of the substrate, with m^* representing the effective mass of the charge carriers (electrons or holes):[3]

$$\omega_p = \left(\frac{4\pi Ne^2}{\epsilon_\infty m^*}\right)^{1/2}. \qquad \text{(Equation 1)}$$

With the largest free carrier densities (10^{22}–10^{23} cm^{-3}), metals (such as Ag, Ag, and Cu) show an accessibility to plasmon resonance in the visible region, and thus are widely adopted as plasmonic substrates for SERS.

Review

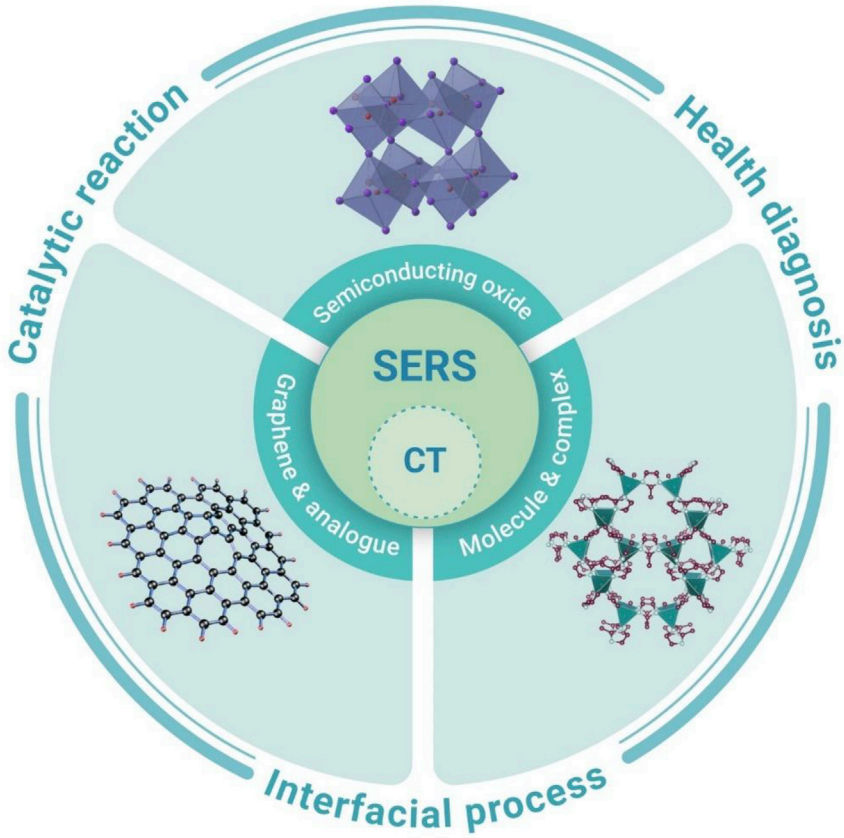

Figure 1. Schematic Illustrating the Charge-Transfer (CT) Induced SERS: Substrates and Applications

Similarly, the adjustable free carrier densities (10^{16}–10^{21} cm^{-3}) in degenerated semiconductors can also support metal-like plasmon resonance and have contributed to the field enhancement when used as SERS substrates, which is discussed later.

The concept of the LSPR-magnified field can be qualitatively derived from the basic physics of the driven harmonic oscillator, as described in an SERS tutorial given by Schlücker.[4] In brief, laser light can be regarded as an external driving force for plasma oscillations in the vicinity of particles, where the resonant elastic light scattering off a metal sphere leads to an increased local field E_{loc} relative to the incident field E_0. The origin of such an enhanced electromagnetic field is the EM-based SERS in plasmonic substrates, which includes the electromagnetic enhancements of both the incident laser and Raman scattering light in two successive steps.[5] The first step is a local field enhancement near the plasmonic nanoparticles at the resonant incident frequency (ω_0), and the second step is a further enhancement of the Raman scattered light when the Raman frequency (ω_R) overlaps with the plasmon resonance (Figure 2A). If the frequencies of the incident laser light and Stokes Raman scattering in the probe molecule are similar, the enhancements to the first and second steps are usually comparable. Therefore, the magnitude of the signal intensity enhancement (I_M) is approximately proportional to the fourth power of the field amplitude (E_{loc}/E_0),[6] which can be expressed by the following equation:

$$I_M = \frac{|E_{loc}(\omega_0)|^2 |E_{loc}(\omega_R)|^2}{|E_0(\omega_0)|^2 |E_0(\omega_R)|^2} \approx \frac{|E_{loc}(\omega_R)|^4}{|E_0(\omega_0)|^4}. \quad \text{(Equation 2)}$$

Notably, such enhancement is independent of the nature of analyte molecules but is determined by the strength of the electromagnetic fields in the presence of plasmonic metal, which can be tuned by modulating the nanostructure morphology, dielectric functions, and the interparticle plasmonic coupling to generate electromagnetic hot spots between neighboring metal particles. Theoretically, the maximum EM enhancement under SERS conditions is 10^{11},[7] which may decrease significantly with increasing distance from the peak value at the shortest junction, and usually varies by orders of magnitude over small distances such as a few molecular dimensions (~2–4 nm).[8] In combined theoretical and experimental studies, Petryayeva and Krull observed a gap-size sensitive variation in the electromagnetic field, with an increased SERS enhancement from 10^5 to 10^9 as the gap between adjacent Au nanospheres decreased from 10 nm to 2 nm (Figure 2B).[9] In fact, even for a uniform molecular distribution on the surface, Raman signals at various locations make different contributions to the exhibited Raman signal, which has been verified by observations that the hottest SERS-active sites represent only 63 out of every 1,000,000 sites, but contribute 24% to the overall SERS intensity.[10]

Metal electrodes (e.g., Ag) roughened by oxidation-reduction cycles were used as the earliest substrates demonstrating the SERS effect, showing a moderate SERS enhancement of about 10^6 for the Raman signals of pyridine.[2] Such electrode-based substrates are usually adopted for *in situ* SERS characterizations of catalytic reactions in electrochemical systems. Today, colloidal metal (Ag, Au) nanoparticles are widely used as substrates for significantly improved SERS activities, based on advances in wet chemical synthesis for controlling the size, shape, or even the arrangement of nanoparticles. SERS effects can be observed with the use of colloidal metals either in suspension or aggregation, both with hot-spot constructions that enhance the electromagnetic field.[11,12] However, due to the non-uniform distribution of nanoparticles with respect to their size and shape as well as the tendency to coagulate, field enhancements based on such randomly produced hot spots (gaps of several nanometers) are usually random, which causes undesirable variation in the SERS signals. To improve the reproducibility of SERS, more complex metal nanostructures with controlled hot spots are prepared using both bottom-up and top-down approaches, such as the assembly of shell-isolated dimers with controllable nanogaps[13] and ordered arrays obtained via lithography.[14–16] Rationally designed plasmon substrates have attracted great research interest for SERS applications.

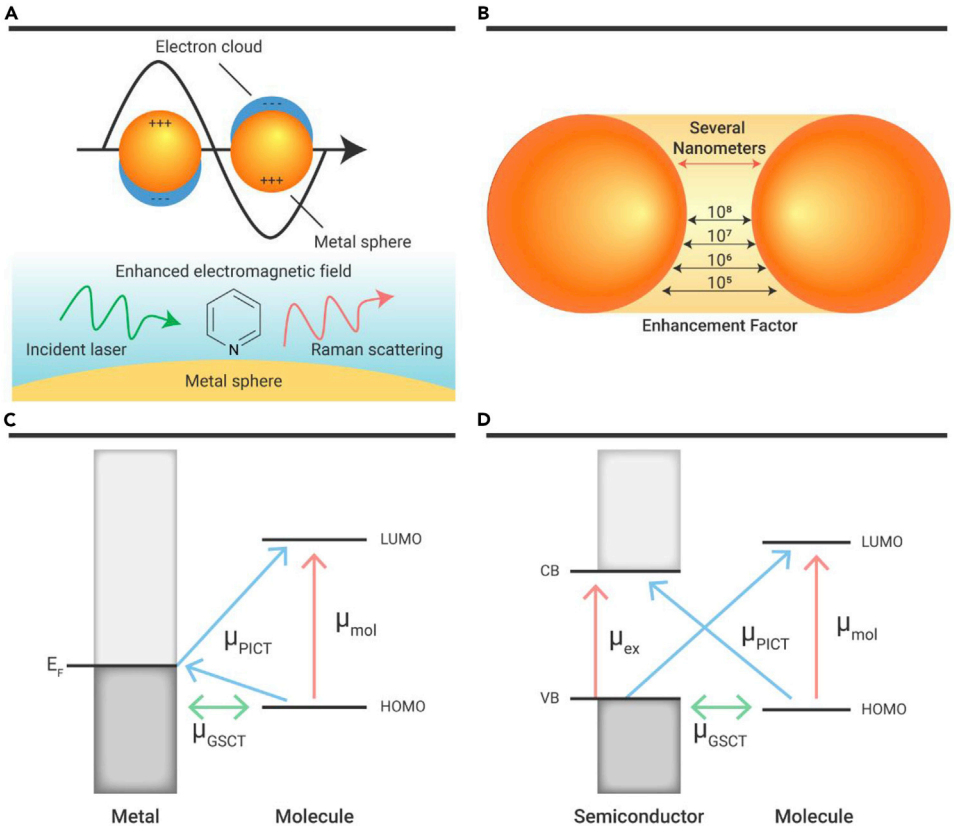

Figure 2. Electromagnetic and Chemical Mechanism for SERS Enhancement. (A) Electromagnetic enhancement in SERS based on plasmonic nanospheres. (B) Schematic illustration of a "hot spot" in the gap between adjacent particles and the corresponding change in SERS enhancement factor with relative positions. Comparison of the charge-transfer transitions in a metal-molecule system (C) and a semiconductor-molecule system (D).

In addition to plasmon resonance, other types of light-matter interactions such as Mie resonance also cause enhancement to the local electric field in the vicinity of the substrate surface. The optical phenomenon of Mie resonance, known as whispering gallery modes or morphology-dependent resonances, is associated with the geometric configuration, which contributes to Raman scattering when the particle size is comparable with the exciting wavelength.[3] With a rational design of the morphology, non-plasmonic dielectrics (such as TiO_2) can be fabricated with enhanced local electromagnetic based on the Mie resonances of the substrate, which can also enable EM-based SERS enhancement.

Chemical Mechanism. Although the EM theory provides a reasonable explanation for the origin of the enhancement in Raman scattering, it fails to clarify the variety of magnitudes of the observed enhancements among different vibrational modes. A CM explaining the enhancement of Raman scattering has also been proposed, whereby the CT in the substrate-molecule system is believed to alter the electron density distribution of molecules, resulting in greater polarizability and thus enhanced Raman scattering. Theoretically, signal amplification via a CM is estimated to reach 10^3 for a model metal-molecular system.[17] To explain the chemical effect in a metal-molecule system, Jensen et al. presented three types of CT contributions, including the interfacial ground-state charge transfer (μ_{GSCT}), the photoinduced charge transfer (μ_{PICT}) resonance, and the electronic excitation resonance within the molecule itself.[18] Figures 2C and 2D show schematics of the three types of contributions to CM enhancements. First, signal enhancement by GSCT is a non-resonant contribution characterized by chemisorption interactions between the molecule and the substrate in the ground state without excitations. Polarizability in the metal-molecule complex can be altered through interfacial CT to yield enlarged intrinsic Raman cross-sections of the complex and fluctuation in the shapes of the Raman spectra. Second, PICT is a wavelength-dependent effect attributed to the CT between substrate and a molecule in resonance with the excitation photons. In a metal-molecule system, this CT can occur in the direction of metal-to-molecule or molecule-to-metal, based on the relative locations of the Fermi level in the metal and the highest occupied/lowest unoccupied molecular orbital (HOMO/LUMO) levels in the molecule (Figure 2C). The largest PICT effect typically occurs when the charge is transferred to/from levels near the metal Fermi level. Third, resonance Raman scattering (RRS) can be involved when the selected laser excitation frequency is close to the electronic transition frequency of the molecule (μ_{mol}) in which RRS can be achieved, usually contributing by a magnitude of 10^2–10^6 to the total Raman signal intensity. The RRS effects are especially noticeable in the case of fluorescent molecules, with increased fluorescence as the main drawback. It should be mentioned that additional CT transitions would also be included as CM contributions in a non-metal substrate, such as the exciton resonance (μ_{mol}) in semiconductors (Figure 2D), in which the electrons can transfer from the valence band (VB) to the conduction band (CB) to create electron-hole pairs known as excitons. The CT scheme in semiconducting materials is similar to that in their metal counterparts but involves separation of the VB and CB by a band gap, with the maximum SERS enhancement at the band edges.[19]

Following the resonance Raman theory developed by Albrecht, a unified perspective to describe all of the CT-related contributions to SERS was proposed by Lombardi and Birke, who introduced the concept of vibronic coupling to the expression of the polarizability.[20] In the mechanism diagram, a probe molecule is covalently bound to a substrate surface to which possible resonance denominators contribute to the SERS intensity, including the surface plasmon, CT, exciton, and molecule resonances. The resulting polarizability (α) can be expressed as the sum of three terms ($\alpha = A + B + C$), with the A term usually considered to be responsible for the RRS, which allows only totally symmetric Raman bands. Terms B and C stem from the substrate-to-molecule and molecule-to-substrate CT transitions, respectively,

which are thought to "borrow" intensity from nearby allowed electronic transitions via vibronic coupling and are involved in non-totally symmetric vibrational modes of the SERS spectra. Accordingly, two requirements are imposed on molecules to achieve efficient CT transitions—one is the covalent bond formed toward the substrate surface to enable charge flow, and the other is the energy-level matching between the molecule and substrate for a strong CT in resonance with incident photons.

Distinguishing the Contribution from Charge-Transfer Enhancement. Large signal enhancements in plasmonic SERS substrates usually arise from the interplay between EM and CM contributions. To obtain a quantitative estimation of the signal enhancement, an average experimental enhancement factor (EF) can be calculated using the following equation:[21]

$$\mathrm{EF} = \frac{I_{\mathrm{SERS}}/N_{\mathrm{SERS}}}{I_{\mathrm{bulk}}/N_{\mathrm{bulk}}}. \qquad \text{(Equation 3)}$$

N_{SERS} and N_{bulk} denote the number of probe molecules that contribute to the signal intensity in SERS and normal Raman spectra, respectively, and I_{SERS} and I_{bulk} denote the corresponding enhanced and normal Raman intensities (Equation 3). As a normal Raman reference, data for a molecule can be acquired using either a bulk molecule solution or a molecule film deposited on a non-SERS active substrate (e.g., SiO_2/Si wafer). Accordingly, the SERS activity of the substrate can be intuitively evaluated by the EF value, but this provides limited information about the relative contributions of the EM and CM effects.

Although CM enhancement from CT processes is ubiquitous in a molecule-substrate system characterized by chemical interactions, it is usually difficult to distinguish when it coexists with EM contributions. Experimentally, spectral signs are recognized as being related to strong CM contributions. For instance, absorption spectra provide clear evidence for the formation of a CT complex between a molecule and substrate, such as the emergence of a weak absorption peak at 1,060 nm for rhodamine 6G (R6G) adsorbed on Ag nanoparticles, which is not present in the individual spectra of the R6G or Ag nanoparticles.[22] The CT contribution can also be recognized by the varied spectral shapes in the SERS relative to normal Raman spectra, with changes in the association of different extents of enhancement between totally and non-totally symmetric vibrations. In fact, based on the variations in relative intensity, CT-contributed enhancement in SERS can be experimentally distinguished. The extent of the CT contribution to the overall SERS signal of a specific Raman band has been described by Chenal et al. with respect to the degree of CT (ρ_{CT}), as expressed in the following equation:[23]

$$\rho_{\mathrm{CT}}(k) = \frac{I^k(\mathrm{CT}) - I^k(\mathrm{SPR})}{I^k(\mathrm{CT}) + I^0(\mathrm{SPR})}. \qquad \text{(Equation 4)}$$

Taken as two reference lines obtained in a Raman spectral region, I^0(SPR) is the intensity of a totally systematic band, and I^k(SPR) is the intensity of the molecular band (k) of concern measured only with respect to the SPR contribution. I^k(CT) is the intensity of band k measured with the CT resonance as an additional contribution to the total SERS intensity. Accordingly, the calculated value of ρ_{CT} is 0 when the system is far from CT resonance and approaches 1 when the CT contributions dominate. In other words, totally symmetric normal modes will dominate the spectrum far from the CT resonance, whereas non-totally symmetric modes become prominent when CT resonances are achieved. Because the resonance contributions in a metal-molecule system (SPR, PICT resonance, and molecule resonance) are all wavelength dependent, determining the contribution of the CT enhancement usually requires a set of SERS data collected at different excitation wavelengths or under varied applied biases. In an example given by Lombardi and Birke,[24] various applied electric potentials were used to evaluate the degree of CT for *p*-aminothiophenol (4-ATP) on an Ag substrate by monitoring the intensity change for the 1,141 cm^{-1} (non-totally symmetric b_2 modes) band (I^k), with the 1,077 cm^{-1} (totally symmetric a_1 modes) band taken as reference (I^0).

The relative intensity among vibrational modes in the SERS spectrum is not only an indication of vibrational mode symmetry but is also affected by the surface selection rules. As is known, a strong component of the electric field normal to the metal surface can usually be induced by SPR while leaving a relatively small tangential component for most molecule-metal configurations. Based on the field-dependent SERS on a metallic surface, the surface selection rule was first conceptualized by Moskovits,[25] who suggested that changes in the molecular polarizability perpendicular to the surface are selectively enhanced, whereas Raman modes oriented parallel to the metal surface are often observed by SERS to have very weak signal intensities. Accordingly, the surface selection rules can provide in-depth diagnosis of the microscopic orientation of molecules anchoring on a metallic surface. For example, as the intensities of the in-plane C–H stretching mode from benzene cannot be observed when the aromatic ring is parallel to the interface, the molecular orientation of small aromatic molecules on gold-aqueous interfaces can be determined by SERS.[26]

Although the SERS enhancement contribution from the CT effect can be experimentally estimated based on the degree of the CT (ρ_{CT}), it remains challenging to separate the CT effects from the plasmon excitations using electronic structure methods, especially via the density functional theory (DFT), due to the poor description of CT states in standard DFT models coupling molecules to metal clusters.[27] Recently, a new visual theoretical method has been adopted that enables the efficient distinction of CM from EM mechanisms. For instance, a quasi-analytical algorithm based on the density functional perturbation theory and the finite difference method was reported by Hu et al., which enables the effective evaluation of Raman tensors in specific molecules adsorbed onto flat Au surfaces.[28] In another example, the charge difference density was used as a theoretical method for visually revealing the resonant CT in a metal-molecule system, with the ability to distinguish PICT resonance, molecule resonance, and EM mechanisms by the charge redistribution between the molecule and metal.[29] A quantitative illustration of the polarizability tensor in SERS was also presented by An et al., who used a combination of analysis methods, with the charge distribution obtained via natural population analysis, the CT interaction energy by natural bond orbital analysis, and a new insight regarding the fragment-to-fragment electron transfer across molecule-metal interfaces based on charge decomposition analysis.[30]

Currently, SERS based on plasmonic metals remains at the core of the field, with the best sensitivity typically obtained by the coexistence of EM and CM contributions. Although the enhancement from CM is often overwhelmed by orders of magnitude by that of EM, it indeed alters the Raman spectral shape based on the interfacial CT transitions, which are especially important in revealing the molecule-substrate interactions. However, in comparison with the relatively well expressed model of the EM effect, the CM contributions in SERS are rather complicated, determined on the basis of interplay of certain CT transitions in the substrate-molecule system. To clearly discriminate the CT-induced SERS effect, plasmon-free materials are used as SERS substrates for observation of the novel structure-function relationship in the SERS effect, based on a primary contribution from CT-induced enhancement.

Graphene and Analogs as Ideal Platforms for Illustrating Chemical Enhancement. Compared with metal, semiconductor materials, especially two-dimensional (2D) semiconducting materials, have unique physicochemical features, including layer-number-dependent band-gap structures, atomic-level flat surfaces, modulable surface sites, and dangling bonds, which greatly facilitate the interfacial CT between the molecule and substrate. Thus, in view of their effective chemical enhancements, 2D semiconductor materials are considered to be promising SERS substrates, three types of which are graphene, transition-metal dichalcogenides, and MXenes.

Graphene Oxide/Reduced Graphene Oxide. Graphene can be understood to be a monolayer of graphite characterized by the packing of carbon atoms into a honeycomb crystal plane. As a semimetal with zero band gap, graphene has excellent physical strength and electron mobility, benefiting from extensive π electron conjugation and delocalization. Because the surface plasmon on graphene is in the terahertz range far from the visible

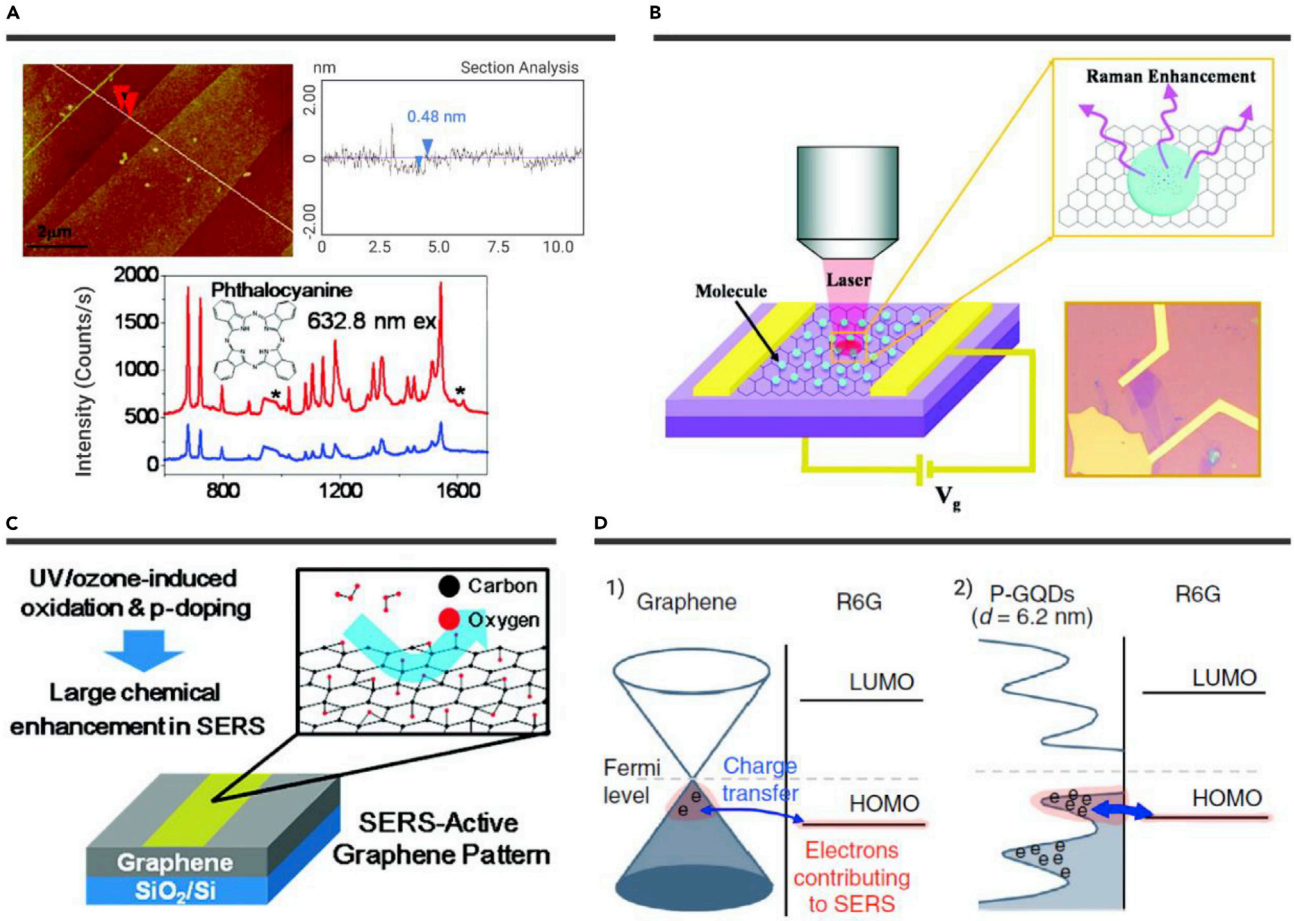

Figure 3. Graphene-Based SERS Substrates. (A) Raman signals of Pc deposited on graphene. (B) Single-layer graphene substrate modulated with electrical field. (C) Graphene substrate by ozone treatment. (D) Graphene quantum dots (GQDs) as SERS substrate. Reprinted with permission from Ling et al.[31] (Copyright 2010, American Chemical Society) (A), Xu et al.[32] (Copyright 2011, American Chemical Society) (B), Huh et al.[35] (Copyright 2011, American Chemical Society) (C), and Liu et al.[36] (Copyright 2018, Nature Publishing Group) (D).

spectrum, as an SERS substrate graphene provides a unique opportunity for the study of CM-based SERS without interference from the EM effect. Ling and coworkers observed a Raman enhancement effect by several common probe molecules (phthalocyanine [Pc], rhodamine 6G [R6G], protoporphyin IX [PPP], and crystal violet [CV]) on the surface of graphene substrates (Figure 3A).[31] Although the calculated EF was only 2–17, taking the Raman signals on an SiO_2/Si substrate as reference, a detection limit (LOD) of 10^{-8} M comparable with that of a metal substrate was obtained for R6G and PPP molecules, with the high sensitivity ascribed to the fluorescent quenching effect by electron- and energy-transfer interactions between graphene and the dye molecules, together with the enrichment of molecules via π-π interaction on the graphene surface. Without interference from EM effects, CT-induced chemical enhancement is clearly evidenced on graphene, featuring a first-layer effect, vibrational mode/molecular-orientation- dependent EFs, and molecule selectivity. Another feature distinct from metal-based SERS is that both the energy-level and structural-symmetry matching between graphene and the probe molecule are important in realizing effective enhancement by the efficient CT between graphene and the molecules.

Since then, efforts have focused on improving the SERS performance of graphene substrates with respect to two basic requirements for CT processes, namely, the surface chemical interaction (first-layer effect) and the energy alignment between the probe molecule and the substrate. The strategy of adjusting external voltages to tune the Fermi level of graphene, as extensively used for metal substrates, was initially used to drive the entire system in/out of CT resonances. By electrical-field modification of the Fermi level of graphene, variation of the Raman intensities of metal phthalocyanine (M-Pc) molecules was achieved (Figure 3B),[32] which were observed to weaken or strengthen when the Fermi level of the graphene was up- or down-shifted, respectively. Thus, energy-level matching between molecules and graphene can be dynamically achieved to ensure effective CT transitions by simply altering the applied potentials. Distinct from metal substrates, graphene (especially in a single or few layers) shows additional potential for a shift in the Fermi level by doping with chemicals. Feng et al. modulated the Fermi level of graphene via controlled nitrogen doping for SERS detection of fluorescent molecules, including rhodamine B (RhB), CV, and methylene blue (MB).[33] Enhanced CT was achieved when the Fermi level of graphene was shifted to align with the LUMOs of the target molecules, leading to significantly amplified Raman vibrational signals that were detectable at concentrations as low as 10^{-11} M. Although ascribed to the CM contribution, the authors found no correlation between the molecule symmetry and the SERS enhancement in the examined probe molecules.

Chemical bonding, also known as the first-layer effect, is another prerequisite for an efficient CT process, which suggests that local chemical groups of the substrate may play an important role in the SERS effect of graphene. Graphene oxide (GO) and reduced graphene oxide (r-GO) are graphene derivatives with different degrees of oxidation, and the active oxygen sites of GO and r-GO have been shown to enhance the affinity toward molecules by chemical bonding. In a comparative study of SERS behavior on graphene, GO, and r-GO, Yang and coworkers obtained a layer-number-dependent enhancement in the Raman signals of an R6G probe.[34] On the graphene substrate, the SERS intensity of the R6G decreased with the increasing numbers of layers of graphene, due to the dominant π-π stacking interactions between

the molecules and graphene. In contrast, a greater SERS effect was observed on the GO substrate as the number of layers increased, which suggests that the oxygenated groups on the GO surface played a significant role. An altered R6G orientation was proposed upon its adsorption onto graphene and GO; however, the exact configuration of the R6G molecules on the surface of the GO was not discussed in this work. Experimentally, surface treatment is effective in the generation of local oxygenized groups on a graphene substrate, such as the UV/ozone-based oxidation method for the treatment of centimeter-scale graphene (Figure 3C).[35] The EFs on the graphene substrate increased from ~10^3 to ~10^4 after ozone treatment using various dye molecules (RhB, R6G, and CV) as probes. The authors suggested that oxygen-containing groups and the p-type doping of graphene could be introduced by surface oxidation, leading to structural disorder and defects on the graphene surface and, thus, a large CT-based Raman signal enhancement.

The size-dependent electronic structure and surface properties in graphene, which have been extensively investigated, would further affect the CT-induced Raman enhancement. Graphene quantum dots (GQDs) as small as 2 nm were obtained directly on SiO_2/Si by Liu et al. using a quasi-equilibrium plasma-enhanced chemical vapor deposition method (Figure 3D).[36] As an SERS substrate, the GQDs had an EF of 2,370 and a sensitivity of 1×10^{-9} M for the detection of rhodamine, which means it was more sensitive than the mechanically exfoliated or chemical vapor deposition (CVD)-grown graphene previously reported. The improved performance was partially attributed to the atomically clean surfaces and large number of edges of the GQDs. The enhanced CT contributions from the GQDs were of equal importance, based on the existence of Van Hove singularities in the electronic density of states (DOS). The use of wet chemical methods demonstrates the feasibility of fabricating GQDs, especially those with controlled doping components, e.g., the nitrogen-doped graphene quantum dots (NGQDs) grown in dimethylformamide (DMF) reported by Das et al.[37] A relatively high SERS sensitivity was observed in NGQDs, which showed an EF of 3.2×10^3 for 10^{-4} M RhB analyte, with the LOD estimated to be 10^{-10} M. The SERS enhancement of the NGQDs was ascribed to a Förster resonance energy transfer together with CM enhancements, which was experimentally isolated by varying the target molecules, laser excitation wavelengths, or functional groups of GQDs.

Although the nature of SERS on graphene and its analogs remains an open question, they have provided plasmon-free platforms for the concrete study of the CT contributions in SERS, whereby the non-resonant GSCT at the interfaces has been found to be in a prominent contributor to the polarization of the adsorbed molecules. It is noted that graphene-based substrates show a metal-comparable LOD for certain analytes, but usually with relatively low EF values, which may be related to graphene's non-polar surface and limited DOS.

Transition-Metal Dichalcogenides. As a family of graphene-like 2D materials, transition-metal dichalcogenides (TMDs) are usually denoted as MX_2, where M represents the transition metals (Mo, W, and Ta), and X the chalcogens (S, Se, and Te). MoX_2 has a layered crystal structure analogous to that of graphene, but with very distinct surface chemical and electronic properties. For instance, molybdenum disulfide (MoS_2), a typical TMD, comprises a layer of Mo atoms sandwiched between two layers of S atoms, with a direct band gap in the monolayer structure but a direct-to-indirect transition in the band structure with an increasing number of layers. The semiconducting electronic structure in MoS_2 is responsible for its SERS behavior, which differs significantly from that of graphene, based on CT-induced SERS enhancement.

A SERS effect on a MoS_2 substrate was reported by Ling et al. in a study comparing hexagonal boron nitride (h-BN) and graphene.[38] MoS_2 and h-BN are typical 2D materials analogous to graphene, but with distinct electronic and chemical properties. Namely, graphene is a zero-band-gap semiconductor with a non-polar surface, BN is highly polar and insulating with a large band gap (~6 eV), and MoS_2 has an indirect band gap and is less polar than h-BN. When using copper phthalocyanine (CuPc) as a probe molecule, Raman enhancement was observed on all three substrates, with the EF values calculated to be 63, 13, and 16 for graphene, h-BN, and MoS_2, respectively. As two distinct processes, the CT on graphene and the dipole-dipole interaction on h-BN were believed to induce an increased electron-transition probability and thus an enhanced Raman signal. Although these two effects might coexist on the MoS_2 substrate, they were too weak to induce a significant SERS enhancement. The observations confirm the importance of CT and dipole-dipole interactions to yield an SERS effect in TMDs. However, SERS sensitivity is still far from satisfactory, nor is there any influence of the structure-function relationship of the TMD substrates (e.g., number of layers, chemical compositions). Subsequently, a system study of layer-number-dependent SERS in TMDs was reported by Meng et al., based on the observation of a layer-controllable WS_2 film synthesized via the CVD method.[39] The monolayer WS_2 exhibited the strongest SERS enhancement toward the R6G probe, but this effect gradually decreased with an increasing number of layers of the WS_2 film. Although the EF value was not calculated, a noble-metal-comparable SERS enhancement was suggested with the monolayer WS_2 substrate, which was ascribed to the clean surface free of any wrinkles or contamination and the controlled thickness/size of the WS_2 substrate, as compared with those obtained by mechanical exfoliation. Moreover, the improved CT obtained with a reduced number of layers might play a crucial role in the Raman enhancement effect due to the indirect-to-direct translation in the WS_2 band structure.

In addition to the adjustable number of layers, the chemical composition or surface atomic arrangement in TMDs can also affect their electronic structure, which is another factor in the significant contribution to the Raman enhancement compared with noble metals. In a recent work by Zheng and coworkers, the SERS sensitivities of various TMDs were significantly enhanced by the incorporation of oxygen into their lattices (Figure 4A).[40] Taking as an example MoS_2, a typical chalcogenide with rather weak SERS activity, oxygen incorporation could be realized either during low-temperature hydrothermal synthesis or by post-thermal treatment in air. The treated samples exhibited a structural morphology similar to that of pristine MoS_2, with a monotonic increase in the lattice oxygen concentration within controlled treatment conditions. It was evident that the proper amount of oxygen incorporation could account for the million-fold magnification in SERS enhancement compared with that of pristine unincorporated MoS_2. This strategy of oxygen incorporation has demonstrated its universality in studies with several other chalcogenide compounds as SERS substrates, which achieved greatly improved performance, including WSe_2, WS_2, and $MoSe_2$. In addition to the featured dipole-dipole interactions, a narrowed band gap with an increased DOS near the Fermi level was observed after "oxygen incorporation" in TMDs, which would facilitate exciton resonance as a further contribution to SERS. In fact, the SERS effects in TMDs may stem predominantly from the excitonic resonance of the semiconductors, as proposed by Muelethaler et al., who observed a high EF of 3×10^5 based on a monolayer MoS_2 substrate for the detection of SERS in 4-mercaptopyridine (4-Mpy) molecules.[41] The large enhancement in the SERS signals was ascribed to the exciton resonance (360–390 nm) of MoS_2 with an unusually high oscillator strength, which would contribute via "intensity borrowing" to the PICT resonance for SERS enhancement.

The SERS activity of TMDs is also dependent on their intrinsic stoichiometric ratios. Liu et al. reported a tailored SERS activity for the detection of CuPc on a CVD-derived WSe_2 monolayer,[42] whereby as the Se/W atomic ratio varied from 2 to 1.92 a 40-fold increase in EF was observed on $WSe_{1.96}$, as compared with that of the pristine WSe_2 substrate. This enhancement was ascribed to the amplified exciton and CT resonance in the molecule-substrate system, which were quantitatively evaluated by femtosecond optical pump-probe analysis and a bipolar junction transistor consisting of CuPc film and the 2D materials. The results showed a 9-fold increase in the quantity of excitons and a 9.4-fold increase in the CT current as the Se/W atomic ratio varied from 2 to 1.92, in accordance with the observed SERS effect. As SERS is an interfacial effect, it is certain that the surficial chemical composition of the substrate is of significant importance to the SERS performances. Thus, aside from the controllable synthesis, post-treatment by high-energy bombardment has also been used as an effective means to boost SERS on TMDs by adjusting the chemical composition or surface atomic arrangement in the layered structure. After oxygen/argon plasma treatment, an improved

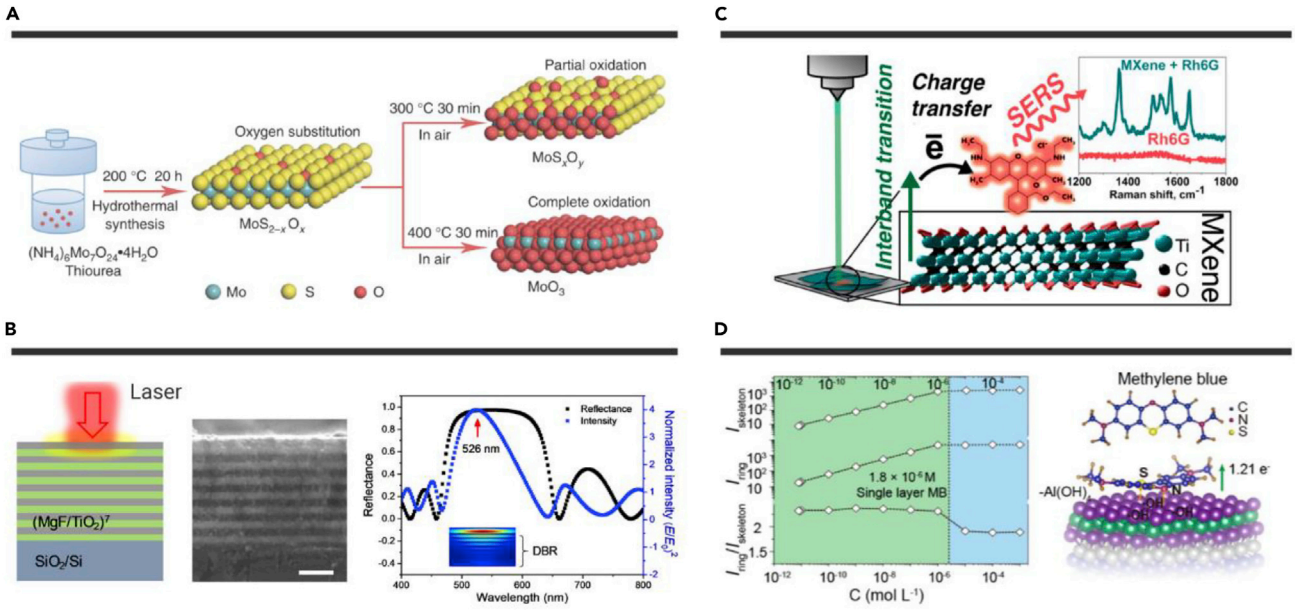

Figure 4. TMD and MXene Substrates. (A) Oxygen incorporation in MoS_2 substrate. (B) 1T′-WTe_2 substrate with distributed Brag reflector (DBR) as field enhancer. (C) Spray-coated $Ti_3C_2T_x$ multi-layered structure as SERS substrate. (D) Al oxyanion functionalized $Ti_3C_2T_x$ substrate. Reprinted with permission from Zheng et al.[40] (Copyright 2017, Nature Publishing Group) (A), Tao et al.[45] (Copyright 2018, American Chemical Society) (B), Sarycheva et al.[50] (Copyright 2017, American Chemical Society) (C), and Li et al.[51] (Copyright 2020, American Chemical Society) (D).

SERS sensitivity on treated MoS_2 (T-MoS_2) of more than one order of magnitude was reported by Sun and coworkers.[43] The enhancement was attributed to the introduction of structural disorders during plasma bombardment, based on the generation of local dipoles and the adsorption of oxygen in ambient air onto dope holes in the MoS_2. The surface oxygen adsorption was considered to decrease the electron occupation at the top of the VB of the MoS_2, which would enhance the PICT between R6G and MoS_2. In another example, femtosecond laser pulses were used to introduce surface micro-/nanofractured structures and S atomic vacancies in monolayer MoS_2. An enhanced physical-chemical adsorption together with interfacial CT was expected after this surface treatment to obtain an enhanced electronic doping effect in the MoS_2 flakes, and a 6.4-fold enhancement was observed in the SERS signals for R6G detection.

Beyond chemical composition modulation, the phase transition of the TMD analogs also plays an important role in their SERS performance. For instance, the semiconducting 2H-phase (with trigonal-prismatic coordination) and the metallic 1T-phase (with octahedral structure) are two typical phases of MoX_2 (X = S, Se) materials, and a transition between the two can lead to different SERS effects based on changes in the electronic structures. Yin et al. observed a significant increase in the SERS effect after a phase transition from the 2H to the 1T phase in MoX_2 (X = S, Se) monolayers, which was attributed to a predominantly CM contribution.[44] After examining the Raman signals of the probe molecules (thermally evaporated CuPc and solution-soaked R6G), the authors suggested that the obviously enhanced Raman signals on metallic 1T-MoX_2 could be ascribed to the facilitated electron transfer from the Fermi level to the HOMO of the probe molecules, which was more efficient than that from the top of the VB for the semiconducting 2H-MoX_2. In fact, the relatively high level of surface activities and high DOS near the Fermi level of the metallic 1T-phase makes certain that TMD materials will rank among the best-performing SERS materials. For example, Tao et al. examined the SERS performance of large-scale 1T′ transition-metal telluride atomic layers grown by the CVD method (Figure 4B).[45] Using R6G as the probe molecule, an efficient CT was observed in WTe_2 with respect to graphene, due to the combined contributions of the high chemical activity of the semimetallic tellurides, strong interface dipole, and the "quasi-covalent bonding" in the R6G-WTe_2 complex, which facilitated efficient fluorescence (FL) quenching and increased the Raman scattering cross-section of the dye molecule. As proof of concept, the WTe_2 sheets were transferred onto a distributed Bragg reflector (DBR) as a field enhancer, which consisted of alternating MgF and TiO_2 layers (both 80 nm thick) grown on a SiO_2/Si substrate. With a 4-fold amplification by the DBR of the field intensity at 526 nm, an LOD as low as 10^{-15} M and a noble-metal-comparable EF of 10^{10} was achieved with the metallic TMD 1T′-WTe_2 substrate. According to Fermi's golden rule, the probability of electron transition is linearly correlated with the DOS around the Fermi level during CT processes. Hence, new types of metallic TMDs with abundant DOS near the Fermi level are now developed as efficient SERS substrates. Song et al. used the CVD method to realize the controllable synthesis of metallic 2D niobium disulfide (NbS_2) nanosheets (<2.5 nm) with a large domain size (>160 μm),[46] and obtained superior SERS activities with respect to other 2D materials such as graphene, 1T-phase MoS_2, and 2H-phase MoS_2. A low LOD of 10^{-14} M and an EF of approximately 10^3 were obtained with an NbS_2 substrate for the detection of an MB analyte, based on the increased intermolecular CT probability. To demonstrate its practical applicability, the NbS_2-based SERS substrates were used for distinguishing between red wines.

In comparison with graphene, TMDs have more complex band structures and abundant surface states, which can support CT-induced Raman enhancement via the contributions of both exciton resonance and dipole-dipole coupling. Until recently, however, the SERS sensitivity on TMD had been considered to be weak due to its limited DOS near the Fermi level. Recent studies have demonstrated significantly improved SERS sensitivity with TMDs, based on the controllable synthesis of the number of layers, the incorporated oxygen, stoichiometric ratio, phase transition, and so forth. The obviously enhanced SERS performances in these TMD substrates are closely related to the abundant DOS near the Fermi level, which facilitates the exciton and CT resonances in the molecule-substrate system. In addition to the traditional family of TMDs, new types of metal chalcogens that exhibit attractive SERS activities, such as $SnSe_2$ nanoflakes[47] and few-layer manganese phosphorus trichalcogenides ($MnPS_{3-x}Se_x$, $0 \leq x \leq 3$),[48] have also been developed, which also stem primarily from the CT-induced enhancement.

MXenes. Another category of 2D materials, MXenes, were discovered in 2011 by Naguib et al.,[49] with the general formula of $M_{n+1}X_nT_x$, where M is a transition metal (e.g., Ti), X is carbon or nitrogen, and T_x represents the

surface terminations (–OH, –F, –O–). Various kinds of MXene materials are developed to obtain distinct physical and chemical properties, from metallic to semiconducting, which shows their great potential as designable substrates for SERS enhancement.

Sarycheva et al. introduced a cost-effective spray-coating method for fabrication of a $Ti_3C_2T_x$ multi-layered structure (with a height of about 300 nm), which obtained SERS enhancement on the order of 10^5–10^6 and analyte selectivity for certain probe molecules (Figure 4C).[50] The SERS activity was ascribed to the combined contributions of the hot spots and the CT facilitated by the $Ti_3C_2T_x$ nanostructures, as evidenced by several experimental observations. The interband CT mechanism was identified by an excitation-dependent spectral feature, as certain R6G bands (~1,528 cm^{-1} and ~1,575 cm^{-1}) were more intensely enhanced by the excitation at 514 nm than at 488 nm. The hot spots' contribution was suggested by the location-dependent spectral feature, as relatively high signal intensities for the R6G bands (614 cm^{-1} and 776 cm^{-1}) appeared at the edges of the MXene island observed via Raman intensity mapping. The chemical selectivity was ascribed to the negatively charged $Ti_3C_2T_x$ surface, which showed affinity toward the cationic MB molecules and repulsion to the anionic acid blue molecules. In fact, the interaction between molecules and MXene nanosheets may be greatly influenced by the electronegative terminations (such as –OH, –F, –O) on the $Ti_3C_2T_x$ surface by frequently disturbing the native structures or conformations of the adsorbed analyte. As a result, there may be changes in the fingerprint Raman spectrum of the target analyte, which is generally undesirable in practical applications of SERS analysis. To solve this problem, Li and coworkers used $Ti_3C_2T_x$ sheets functionalized with aluminum oxyanion groups as substrates and achieved a highly sensitive but non-selective SERS enhancement (Figure 4D).[51] The Al-oxyanion-functionalized $Ti_3C_2T_x$ substrate was found to be sensitive to a series of analytes including dye molecules such as MB, R6G, brilliant green, methyl green, CV, and Nile blue, as well as harmful chemicals such as Sudan III, 1,10-phenanthroline monohydrate, 4-aminobenzoic acid, and 4-mercaptobenzoic acid (4-MBA), with an LOD close to the picomolar level. The surface Al oxyanion functionalities of the $Ti_3C_2T_x$ substrate were demonstrated to play critical roles in inducing strong but non-selective interactions with analytes. The analytes, especially those with low concentration, could adopt a configuration similar to that on a blank substrate, lying flat with the C–N slightly distorted toward the substrate, which enabled the unusual combination of high sensitivity and enhancement of the signals while showing no obvious preference among different vibrational modes. In an example reported by Ye et al.,[52] however, the large number of hydroxyl radicals and crystal defects on the surface of $Ti_3C_2T_x$ were believed to hinder the CT and SPR effect of SERS. Using the chemical exfoliation method assisted by microwave heating, monolayer Ti_3C_2 nanosheets were obtained with improved crystallinity and the elimination of surface hydroxyl groups, which exhibited a maximum EF of 3.82×10^8 and an LOD of approximately 10^{-11} M for environmental pollutants such as azo dyes, trichlorophenol, and bisphenol A (BPA). Based on the 2D electron gas distribution in the Ti_3C_2 monolayer, the SERS enhancement was ascribed to the contributions from both a strong LSPR and a significant interfacial CT, as revealed by DFT calculations.

The reduction of MXenes can also be used to tailor the SERS enhancement, as demonstrated in a recent work by Limbu et al.[53] Reduced $Ti_3C_2T_x$ MXene nanosheets (r-$Ti_3C_2T_x$), obtained by treatment with L-ascorbic acid, showed an EF of 10^7 for R6G detection, an order of magnitude larger than that of pristine $Ti_3C_2T_x$ substrate. The improved SERS activity of r-$Ti_3C_2T_x$ was ascribed to the efficient interaction and CT between the MXene surface and the probe molecules, which benefited from the removal of the F terminations (more than 50%) and the large exposure of the surface Ti atoms upon reduction. In addition, an increased DOS at the Fermi level of r-$Ti_3C_2T_x$ would facilitate the CT processes, which would also contribute to the enhanced Raman signals. Unlike the observations by Ye et al.,[52] the authors of this study did not suggest the involvement of EM contributions in their system, as no plasmonic absorption was observed in the visible region, despite the presence of metallic features or increased DOS at the Fermi level of r-$Ti_3C_2T_x$. In comparison with carbide MXenes, an even larger DOS at the Fermi level can be obtained with nitride-based MXenes, which feature high electronic conductivity and which may also influence the SERS activity. Soundiraraju and George reported the fabrication of a paper-based SERS substrate using few-layered Ti_2NT_x and achieved a high EF of 10^{12} for R6G detection.[54] The Raman signal enhancement in the presence of Ti_2NT_x MXene was ascribed to the high electron density distribution on the N atoms, due to their electronegativity with respect to the C atoms in carbide-based MXenes. With no shift observed in the peaks of the SERS spectra, an EM-dominated enhancement mechanism was suggested based on the bent and curved surfaces of MXenes that served as hot spots, as evidenced from the atomic force microscopy and field-emission scanning electron microscopy results. Benefiting from the high specific area of the analyte accumulation, the SERS efficiency of the paper substrate was further demonstrated by the detection of explosives such as PETN, HMX, and RDX.

As a newly developed family of 2D materials, MXenes are attractive candidates as SERS substrates due to their rich electronic DOS at the Fermi level and abundant electronegative groups on the surface, which will support the contributions of both EM and CM to the enhanced Raman signals. Although the underlying mechanism for the SERS effect in MXenes is still under debate, MXene-based substrates with high sensitivity and certain fascinating advantages have already been developed, such as spectral-shape preservation and analyte selectivity.

Semiconducting Oxides as SERS Substrates with Boosted Activities. Transition-metal oxides constitute a large variety of semiconducting materials that have a surface electronic structure easily modified due to the multivalent nature of the transition-metal ions as well as the high reactivity of the oxygen element. Benefiting from the allowed CT between the molecules and oxides, which can be modulated in resonance with incident photons, an SERS effect would be expected from these oxide substrates. In recent years, boosted SERS sensitivity comparable with that of plasmonic metals has been reported for various transition-metal oxides, and the use of semiconducting oxides as SERS substrates has quickly become a hot topic in the SERS field from both theoretical and practical viewpoints.

Oxides of Titanium and Zinc. Titanium oxide (TiO_2) and zinc oxide (ZnO) are two typical wide-band-gap semiconductors with similar band-level locations and energy gaps (~3.2 eV) for absorption in the UV region of the spectrum. These two semiconducting oxides were once extensively studied as photocatalysts based on their excellent optical and surface chemical properties, which made them among the initial candidates for the investigation of semiconducting SERS. A detailed study of the SERS effect on TiO_2 in 2008 was reported by Yang et al.,[55] in which the SERS enhancement of several mercapto aromatic molecules, i.e., 4-MBA, 4-Mpy, and 4-ATP, was attributed to the TiO_2-to-molecule CT facilitated by the increased electron-attracting ability of para-groups to the mercapto group chemically bonded to the TiO_2 surface. However, this CT-induced enhancement was not totally supported by Musumeci et al.,[56] who agreed with the need for the formation of a CT complex between the molecules and TiO_2 but proposed a reversed CT route of molecule-to-TiO_2 contribution to the SERS enhancement, as demonstrated using dopamine, salicylate, acetylacetone, and benzoate as analytes. A CM enhancement on the TiO_2 substrate was suggested by the calculated EF (~10^3) approaching the predicted maxima, evidenced by features of CT-induced SERS such as wavelength-dependent intensities, enhancement of selected vibrations, and the appearance of new bands. However, the authors suggested that more work was required to address the details of the enhancement mechanism.

To improve the sensitivity of plasmon-free semiconducting substrates such as TiO_2 and ZnO, the strategy for designing sub-wavelength photonic structures was initially based on enhanced light-matter coupling. Qi and coworkers applied an inverse opal photonic microarray as the SERS substrate, with the SERS sensitivity modulated by carefully matching the laser wavelength to the photonic band gaps of the microarray.[57] An optimized SERS sensitivity comparable with that of plasmon metal (without the aid of a

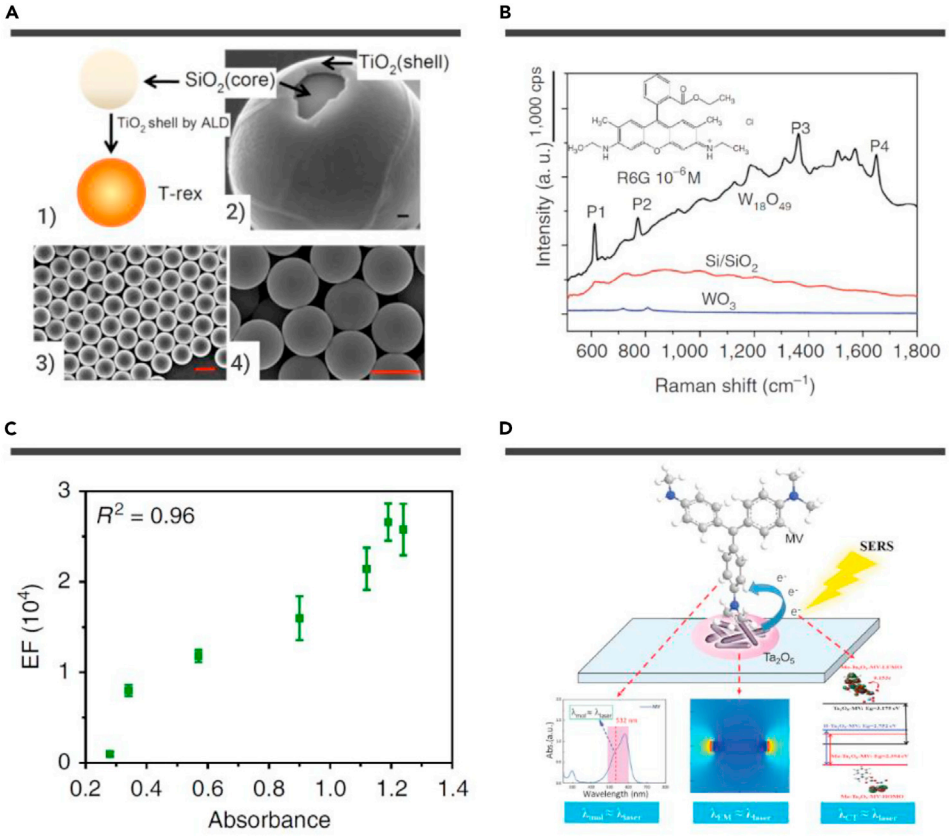

Figure 5. Semiconducting Oxides as SERS Substrates. (A) TiO_2 shell-based resonators. (B) Oxygen-defect engineering strategy for boosted SERS in tungsten oxide. (C) Electrochromic SERS substrate with high reproducibility. (D) Mechanism diagram of the "coupled resonance" strategy on the Ta_2O_5 substrate. Reprinted with permission from Alessandri[58] (Copyright 2013, American Chemical Society) (A), Cong et al.[67] (Copyright 2015, Nature Publishing Group) (B), Cong et al.[76] (Copyright 2019, Nature Publishing Group) (C), and Yang et al.[83] (Copyright 2019, John Wiley & Sons, Inc.) (D).

hot-spot effect) was reported for this TiO_2 photonic microarray, with an LOD of 6×10^{-6} M and an EF of 2.0×10^4 for MB molecules. The improved SERS of TiO_2 is related to the enhanced light-matter interaction by the repeated and multiple light scattering in the photonic microarray. In another example by Alessandri,[58] a cavity structure was used to improve the SERS effect on a semiconductor via the Mie resonances, where the total internal reflection within the dielectric microspheres gave rise to evanescent electromagnetic fields that also generated local hot spots (Figure 5A). Monodispersed SiO_2@TiO_2 core/shell microspheres, known as T-rex, were synthesized by coating the SiO_2 microspheres with conformal shell layers of amorphous TiO_2 of various thicknesses (ranging from 5 nm to 100 nm) via atomic layer deposition. The improved SERS on T-rex compared with a planar TiO_2 film substrate was due to the synergistic effect of a high refractive index in the shell layer, multiple light scattering through the spheres, and related geometrical factors in the designed photonic resonators. With the T-rex structure, Bontempi et al. achieved the first plasmon-free SERS detection of environmental CO_2, a small molecule known to have an extremely low Raman cross-section ($\sim 10^{-30}$ cm^2 sr^{-1}),[59] for which the SERS effect was confirmed using a computer code implementation of the Mie theory (SPLAC). In addition to the field enhancement provided by the T-rex structure, the adsorption of CO_2 molecules onto the TiO_2 shell layers of the T-rex beads from both the air and water/alcohol solvents also plays an important role in this detection. This superstructure design strategy was also applied to ZnO, as reported by Ji et al., to achieve a synergistic effect between the CT and Mie resonances.[60] The spherical ZnO superstructure with a uniform diameter ranging from 220 nm to 490 nm was produced by the aggregation of primary single crystallites approximately 13 nm in size, which had an EF value of 10^5 for a nonresonant molecule (4-Mpy) probe. By calculating the field enhancement using Mie theory, followed by moving the excitation from 532 nm to 633 nm and 785 nm to rule out PICT contributions, the EF values of the Mie resonance, PICT resonance, and GSCT were differentiated to be 10^2, 10^2, and 10, respectively.

As is well established in photocatalysis, TiO_2 in different phases (e.g., anatase and rutile) will vary in its physicochemical properties, such as band gap and adsorption ability toward foreign molecules. A synergistic effect featuring improved photophysical and photochemical activities can typically be achieved in mixed-phase TiO_2 based on a favored charge-carrier transport and separation. These phase-determined properties may also be beneficial to plasmon-free SERS enhancement. Yang and coworkers synthesized TiO_2 nanoparticles in anatase, rutile, and their mixed crystal phase using a sol-hydrothermal method.[61] When compared with single-phase TiO_2 as the SERS substrate, the mixed-phased TiO_2 crystal with an appropriate anatase/rutile ratio showed stronger SERS enhancement for 4-MBA detection, which was explained by the TiO_2-to-molecule CT contribution. In fact, the SERS effects in semiconductors are not only determined by the phase structures but can vary among different facets within a single crystalline phase. Yu and coworkers reported the facet-specific SERS of anatase TiO_2, based on the synthesis of sea urchin-like TiO_2 substrates with high-index (201) facet exposure, which they obtained hydrothermally using acetic acid and DMF as facet direct agents.[62] The authors obtained an SERS EF of 1.6×10^6 with this (201) facet-dominant substrate for dopamine detection, which is three orders of magnitude higher than those of TiO_2 with (101), (001), and (100) facets, with the observed SERS performance ascribed to the greatest CT between dopamine and the (201) facet with a high density of unoccupied t_{2g} orbitals.

In view of the interfacial CT process between semiconductors and molecules, the ordered periodic lattices in crystalline materials generally constrain the electrons, and the long-range disordered structure in

amorphous materials may result in metastable energy states that facilitate escape by the surface electrons. Wang et al. reported an EF of up to 6.62×10^5 on an amorphous a-ZnO nanocages (a-ZnO NCs) substrate for the detection of mercapto molecules.[63] The authors attributed this remarkable SERS sensitivity to an enhanced interfacial CT process by the metastable electronic states in a-ZnO NCs, as indicated by the generation of π bonding in the Zn–S bonds of the mercapto molecules adsorbed onto the a-ZnO NCs. Such a phase-related SERS enhancement was also observed for TiO_2.[64] On a 2D amorphous TiO_2 nanosheets (a-TiO_2 NSs) substrate, a high EF of 1.86×10^6 was obtained for 4-MBA (10^{-4} M) molecules, with the CT in the substrate-molecule complex again found to be the primary contribution, facilitated by a large number of surface oxygen deficits and a low coordination number of surface Ti atoms on the amorphous 2D surface. In fact, semiconductor nanocrystals with reduced size dimensions vary significantly in their electronic structures and surface coordination, which would contribute to SERS based on CT-induced contributions. Recently, a noble-metal-comparable SERS enhancement efficiency was reported by Dharmalingam et al. on the basis of a low-dimensional TiO_2 substrate that featured a high concentration of atomic-scale defects on the surface.[65] Using ultrafast femtosecond pulsed laser ablation, the authors obtained quantum-sized non-plasmonic TiO_{2-x} particles, which showed an extremely high EF of ~10^{10} and a low LOD of 10^{-9} M for the CV molecule. The quantum-sized TiO_2 was also demonstrated to be effective in the SERS detection of cancer biomolecules (ATP and EGFR peptide) with low Raman cross-sections, showing wavelength-independent sensing and long-term activity. The authors excluded an EM contribution in the substrate, and attributed the high SERS sensitivity to the excellent CT enabled by the enriched electronic states and high density of the defects on the quantum-sized nanoparticles.

Oxides of Tungsten and Molybdenum. Tungsten and molybdenum are two typical group-VIB metals in the periodic table of elements, which have similar atomic radii and variable valences ranging from +6 to +4 in their oxides. Based on the common construction from MO_6 (M = W, Mo) octahedra, there are physicochemical similarities in the oxides of tungsten and molybdenum, including oxygen-deficit structures, high carrier densities, and a corresponding absorption related to SPR. For instance, the existence of substoichiometric tungsten oxide indicates that the basic structure of WO_3 could extend to the composition $WO_{2.9}$ with self-doping of the oxygen vacancies. Since then, numerous stable substoichiometric examples, documented as Magnéli phases, have been experimentally recorded with the composition of WO_x (x varies from 2.625 to 2.92) featuring edge-sharing WO_6 octahedral units to eliminate lattice oxygen sites.[66] Although tungsten oxide has been intensively utilized as a versatile optoelectronic material, with its application in sensors, electrochromic/photochromic devices, photothermal/photodynamic therapy, and visible-light driven photocatalysis, it has been rightfully recognized as an SERS-inactive material.

In 2015, Cong and coworkers first demonstrated a greatly enhanced SERS effect based on a defect-rich semiconducting oxide material (Figure 5B).[67] By creating surface oxygen vacancies via H_2/Ar thermal reduction, the SERS activity of the $W_{18}O_{49}$ substrate could be effectively improved, with a maximum EF of 3.4×10^5 and an LOD as low as 10^{-7} M for the R6G analyte. This astonishing enhancement ranked tungsten oxide as a high-performance semiconducting material comparable with noble metals without rationally designed hot spots. As an initial work, the results have demonstrated the importance of oxygen vacancies to the SERS activity of tungsten oxides, with the proposed SERS enhancement of semiconductors based on the CT contributions of the semiconductor-molecule system. Deep levels in the band gap introduced by "oxygen extraction" can act as a springboard to facilitate both the charge-carrier generation and transportation, increase the polarization tension of the adsorbed molecule through vibronic coupling, and finally increase the Raman signals. It is fascinating that the SERS activity of semiconductor oxides can be dramatically promoted by the suitable modulation of the lattice oxygen density, which means that the oxygen-defect engineering method may resolve the limitation of active substrates in SERS applications to provide a universal strategy for boosting the SERS activity of common semiconducting oxides. Similarly, Fan and coworkers integrated non-stoichiometric and amorphous features in WO_{3-x} thin films, which showed an EF up to 10^7 and an LOD of 10^{-9} M for R6G.[68] The authors excluded possible EM contributions, as the LSPR of WO_{3-x} could hardly be excited at the excitation wavelength of 532 nm. Instead, a promoted PICT resonance was believed to be the reason for the observed SERS enhancement, benefiting from the narrowed band gap, the defect levels generated within the band gap, the strong exciton resonance, and the high electronic DOS near the Fermi level of the WO_{3-x} substrate.

Wu and coworkers extended this oxygen-defect engineering strategy to hydrothermally prepared α-MoO_{3-x} nanobelts, and proposed a comprehensive model for the oxygen-defect-induced PICT process.[69] By introducing oxygen deficits, non-SERS active α-MoO_3 was endowed with SERS activity for the detection of 4-MBA, MB, and R6G, with an EF reaching 1.8×10^7 and an LOD as low as 10^{-8} M. Based on experimental observations, the PICT between the absorbed molecules and the semiconductor was believed to be the main reason for the SERS enhancement, as described by an effective electric current model. Cao et al. also applied a facile reduction method to modulate the oxygen vacancy concentration in oxide SERS substrates.[70] By controlled reduction with metal lithium, the authors obtained a MoO_{2-x} nanosphere product with adjustable oxygen deficits. A plateau in the Raman enhancement with an LOD of 10^{-8} M for R6G was observed on the 6-wt % Li-treated MoO_{2-x} substrate, which was ascribed to the saturated promotion effect of the CT in relationship with oxygen deficits in the MoO_{2-x} samples.

With the formation of oxygen vacancies and non-polar metallic bonds (e.g., W–W, Mo–Mo) in the lattice, free-electron gas can be accumulated to a large density (~10^{21} cm^{-3}) in the surficial region of tungsten/molybdenum oxides, even approaching that of metals.[71] Therefore, some metal-like properties can be observed with these oxygen-deficit oxides, including LSPR at various frequencies. Wang et al. synthesized oxygen-deficit MoO_{3-x} nanosheets by a redox reaction between MoO_3 nanosheets and dopamine, which showed multicolor and tunable LSPR from the UV to near-infrared region (361–809 nm) by varying the pH values of the medium.[72] The PDA-coated MoO_{3-x} showed high SERS sensitivity toward R6G probe dye, with an LOD as low as 0.3 fM and an EF magnitude of 10^{10}, in which molecular resonances coupled with the interfacial CT were suggested to contribute to the strong SERS effect. However, the LSPR-induced EM contribution was excluded by the authors, based on a comparison of the colored substrates with different LSPR locations. They observed that the most active substrate (blue) depicted LSPR with no absorption overlap, and the substrate (yellow) with high carrier density showed weak SERS activity.

Whether an EM enhancement is contributed in substoichiometric tungsten/molybdenum is still under debate, due to variations in the synthetic method, substrate morphology, and Raman measurement (e.g., laser wavelength, probe molecules). Some researchers have suggested that substoichiometric tungsten/molybdenum oxides could be endowed with metal-like SPR together with inherent CM enhancement as an explanation for their unexpected high SERS sensitivity. For instance, large-area hexagon plum-blossom-like WO_{3-x} nanoarrays fabricated on an aluminum nanobowl array were used as an SERS substrate by Hou et al.,[73] which showed a low LOD below 10^{-9} M for R6G analyte, which they ascribed to a coupling enhancement between LSPR and PICT. Zhang and coworkers synthesized a series of oxygen-deficit tungsten/molybdenum oxide hierarchical nanostructures that feature quasi-metal properties such as strong LSPR absorption in the visible region. Such plasmonic semiconductors have been observed to have high SERS sensitivities toward multicomponent detection due to synergistic contributions of an EM and CM. MoO_2 with nanodumbbell and nanosphere morphologies were also synthesized, which showed a minimum detectable concentration of 10^{-8} M and a maximum EF up to 10^6 with R6G as a probe.[74] For practical applications, MoO_2 hierarchical nanostructures were demonstrated to be effective in the detection of high-risk chemicals such as BPA, dichlorophenol, and pentachlorophenol, and for multicomponent samples containing R6G, MB, and methyl orange (MO) at a concentration of 10^{-6} M. Similarly, hierarchical WO_2 hollow nanodendrites with large surface areas were synthesized, which showed SERS sensitivities exceeding their own MoO_2 counterpart, with an EF of 8.5×10^7 and an LOD

of 10^{-10} M reported for an R6G analyte. Furthermore, as a demonstration of practical application, patterned SERS chips based on WO_2 nanodendrites were fabricated by nano-ink spraying, which realized the separation, enrichment, and detection of multicomponent samples.[75]

Besides the sensitivity of SERS detection, reproducibility of the Raman signals, and reusability of the substrate, other important criteria must be met before real-world applications can occur. Although striking EFs have been achieved with tungsten-/molybdenum oxide-based substrates, constructing SERS substrates with excellent reproducibility and renewability remains a great challenge, especially with respect to the defect engineering strategy, which often requires careful experimental designs and sophisticated processes. Recently, Cong and coworkers succeeded in finding an attractive strategy to ensure the reproducibility and renewability of SERS substrates based on the electrochromic effect (Figure 5C).[76] Electrochromism is a typical phenomenon whereby transition-metal oxides reversibly alter their optical outlook between transparent and colored states upon ion/electron insertion/extraction by driving the bias potentials. This unique phenomenon has been actively researched for "smart" windows, displays, and other cutting-edge applications, but has never been proposed to overcome critical problems in the field of SERS. The possibility of this combination is based on a unique quantitative relationship between the SERS signal amplification and the degree of coloration, in which the SERS activity of the substrate can be effectively inferred by judging the degrees of color. In practice, the colored substrate showed a strikingly increased SERS enhancement by a factor of 28 relative to the pristine uncolored film, with a record low batch-to-batch relative standard deviation (RSD) of 6.79% and a run-to-run RSD of 2.52%, which indicates the excellent reproducibility and renewability of the electrochromic SERS substrates. The unique colorimetric enhancement in SERS was derived from the quantitative control of the filling of the d-orbital electrons during the electrochromic process, showing a linear dependence on the DOS near the Fermi level, thus dramatically affecting the Raman scattering polarizability of the analytes. The results may provide a first step toward the rational design of electrochromic SERS substrates with high sensitivity, reproducibility, and renewability, which are urgently desired for the quantitative analysis, standardized production, and low cost of SERS substrates. Apart from the quantitative insertion of cation/electrons via electrochromic processes, precise defect control in tungsten oxide can also be realized by electrical tuning, as reported in a recent work by Zhou et al.[77] An electric field was used to introduce defects in a substrate fabricated by WO_{3-x} nanoparticles spin-coated between two Au planar electrodes on a Si wafer, which showed a tuned SERS EF range for RhB from 3.01×10^5 to 1.14×10^6. Based on the electrical programming of defect density, defect levels introduced by the oxygen vacancy could be well aligned to the molecular levels, thus facilitating CT between the substrate and molecules.

Oxides of Copper and Group-VB Metals. Cu_2O was first documented as an SERS substrate by Kudelski and coworkers in 1998, who observed the characteristic SERS signals of pyridine on Cu_2O-coated copper electrodes.[78] Jiang et al. reported the fabrication of Cu_2O nanoparticles with various morphologies via wet chemical methods for their application as dielectric SERS substrates that exhibited near-field EM in close relationship with the structures. For instance, Cu_2O nanospheres were synthesized via controlled deposition directed by the triblock copolymer Pluronic P123.[79] Benefiting from the S–Cu bonding between the mercapto molecules and semiconductor, the Cu_2O nanospheres showed SERS activity for 4-MBA and 4-Mpy molecules, with an estimated EF of $\sim 10^5$. Contributions from both CM and EM were responsible for the SERS enhancement in the Cu_2O substrate, with the former evidenced by the enhancement in the non-totally symmetric modes of the analyte and the latter by the enhanced electromagnetic field around the rough Cu_2O nanospheres via theoretical simulations. In another example,[80] very complicated nanostructures of Cu_2O were designed to achieve improved light-matter interaction, with Cu_2O spheres with controllable concavity synthesized using a "temperature-induced stacking" strategy. The designed Cu_2O concave spheres showed an ultralow LOD of 2×10^{-8} M and a metal-comparable EF of 2.8×10^5 for an R6G probe, which was ascribed to the effective light-trapping/-scattering effect in the cavity enclosed by walls, together with the CT-induced enhancement. A defect engineering strategy to boost SERS has also been verified with copper oxide, just as that initially observed using tungsten oxide materials. A three-dimensional (3D) cube-like Cu_2O superstructure was constructed with a large number of defects, which resulted in the generation of new surface states that facilitated the PICT in the semiconductor-molecule system.[81] Without the EM contribution, however, a metal-comparable EF of 8×10^5 and a low LOD of 10^{-9} M (R6G) were also observed with a Cu_2O superstructure, based on a CT-dominant SERS enhancement.

The elements V, Nb, and Ta are three common representative group-VB metals in the periodic table of elements, whose corresponding oxides are widely exploited in the fields of catalysis, electronics, and optoelectronics, which benefit from their adjustable band structures and rich surface sites. For instance, niobium pentoxide (Nb_2O_5) is a wide-band-gap semiconductor characterized by the sub-coordination Nb^{5+} ions (Lewis acidic sites) and electro-rich hydroxyl species (Brønsted sites) on its surface. By directly using commercial Nb_2O_5 nanoparticles as the SERS substrate, Shan and coworkers observed an extraordinarily high EF of more than 10^7 for MB detection.[82] Both CM and EM contributions were suggested, with the former evidenced by the significant shifts in the location of several bands and the latter analyzed by the finite element method. In another work by Yang and coworkers,[83] Mo-doped Ta_2O_5 nanorods were hydrothermally synthesized, which showed high SERS sensitivity, with an EF of up to 2.2×10^7 and an LOD of 9×10^{-9} M for a methyl violet (MV) probe (Figure 5D). This remarkable enhancement was attributed to certain resonances, including the molecular resonance of MV, PICT resonance, and electromagnetic enhancement around the "gap" and "tip" of anisotropic Ta_2O_5 nanorods. Benefiting from the photocatalytic activity of Ta_2O_5, the substrate also demonstrated a self-cleaning capability.

As an interesting transition-metal oxide with intermediate valence states, vanadium oxide has various polymorphs with significantly modulable physicochemical properties. Based on the oxygen-defect engineering strategy, boosted SERS activity in V_2O_5 was observed by Wu et al., based on improved PICT processes between the semiconductor substrate and adsorbed molecules.[69] Recently, metal-comparable SERS sensitivity was observed in VO_2 nanosheets, which showed a maximum EF of 6.7×10^7 and an LOD for R6G at the 10^{-10} M level.[84] A detailed step-by-step study of the components contributing to the SERS enhancement was introduced in this work. For instance, the existence of electrostatic coupling was explained by the strong dipole effect and quasi-covalent bonds between VO_2 and R6G, the PICT was supported by the energy-level matching between the VO_2 and R6G molecule, and the EM was evidenced by the SPR-related SERS performance. By evaluating the intensities of non-totally symmetric modes recorded on VO_2 and SiO_2-coated VO_2, the CM and EM contributions were estimated to be 57% and 43%, respectively.

In recent years, SERS based on semiconducting oxides has witnessed rapid development, with boosted signal sensitivities approaching those obtained with plasmonic metal substrates. The SERS performance is largely related to the inherent modulability of these oxides, either morphological or compositional, which then leaves the arduous task of clarifying the exact origin of the enhancement. The structural features of the oxides, i.e., morphology, size, phase, facet, and defects, have all been proved to be responsible for the SERS enhancement observed with these semiconducting oxides. Cooperative resonance effects could be induced by rationally designed oxide structures, including exciton resonance, molecular resonance, molecule-semiconductor CT resonance, and even electromagnetic resonance including metal-like SPR and the Mie scattering resonance of semiconductors under a laser excitation. An optimized SERS enhancement in semiconducting oxide substrates would be achieved by a reasonable selection of the semiconductor-molecule system and an excitation wavelength based on an efficient interfacial CT.

Organic Molecules and Complexes as SERS Substrates Show Versatile Tenability. Recently, molecular compounds and organic-metal complexes with SERS activity have been observed. In comparison with their inorganic counterparts, the organic components in the substrate play an indispensable

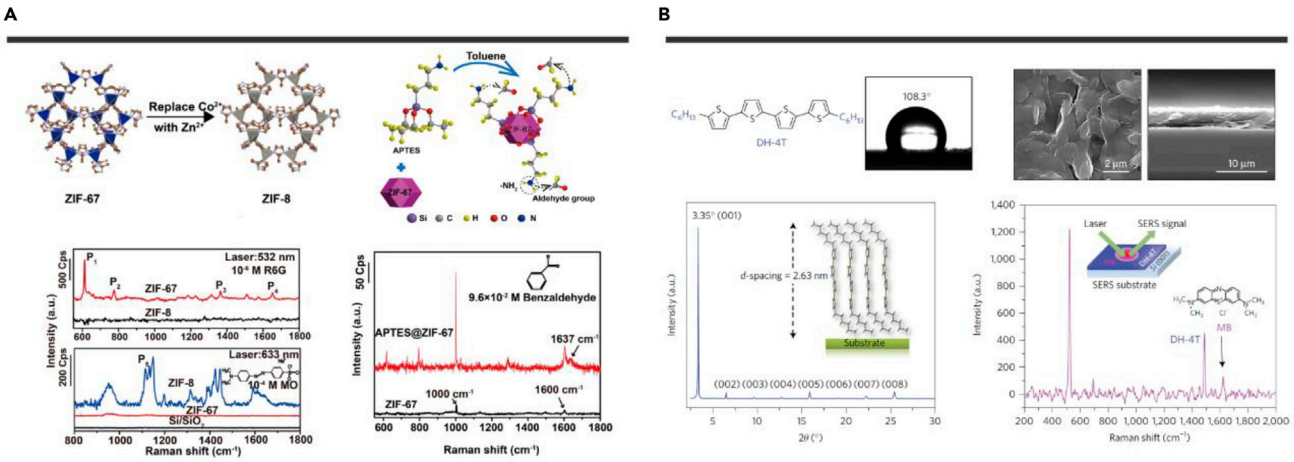

Figure 6. MOFs and Conjugated Molecules as SERS Substrates. (A) MOF substrates with high tailorability. (B) Nanostructured organic semiconductor films. Reprinted with permission from Sun et al.[85] (Copyright 2019, American Chemical Society) (A) and Yilmaz et al.[88] (Copyright 2017, Nature Publishing Group) (B).

role, especially in view of the CT-induced SERS enhancement. Benefiting from the versatile tunability of both the carbon backbones and functional groups of organics, chemical binding toward specific target molecules is facilitated on the substrate, which promises further Raman signal enhancement. Organic molecules and complexes with SERS activities are all featured by their semiconducting nature, which can be roughly divided into three categories: metal-organic frameworks, organic-inorganic hybrid perovskites, and conjugated organic semiconductors.

Metal-Organic Frameworks. Metal-organic frameworks (MOFs) are a typical class of hybrid organic-inorganic supramolecular materials that contain 3D and periodic networks of metallic nodes held together by bridging organic linkers. The discovery of MOFs triggered great and enduring excitement in various fields, including chemistry, physics, materials science, engineering, and biology. SERS is an interesting application area of MOFs worthy of exploration based on their unique characteristics. For instance, the significant structural flexibility of MOFs makes it enticing to pursue metal center/organic linkers and topological designs that selectively maximize the interfacial CT interactions to enhance SERS signals. Generally, MOF materials are known to be good scaffolds for noble metal particles, which benefit from their ultrahigh specific surface areas and modulable pore interiors and may facilitate the enrichment of target molecules and lower the LOD, with the noble metal particles making major contributions to the SERS activities. Sun and coworkers demonstrated that MOF materials could serve as a type of molecular-selective SERS substrate capable of remarkable Raman EFs (~10^6) and a low LOD (~10^{-8} M) for specific analytes (Figure 6A).[85] One of the most intriguing features of the MOF SERS substrates is their high tailorability. By adjusting the metal centers and organic ligands, the electronic band structures of an MOF-based SERS substrate can be purposively manipulated to match the target analyte, resulting in the combination of several resonances, including the PICT resonance, interband transition resonance of the MOFs, and molecular resonance, with subsequently significant SERS enhancement. For instance, ZIF-8 is an isomorph of ZIF-67 prepared under similar growth conditions by the replacement of the central Co ion with a Zn ion, but suitable for different types of SERS analytes. Based on the observations, ZIF-67 is an SERS-active substrate for R6G (10^{-6} M) when excited at 532 nm, whereas ZIF-8 is non-SERS active in this situation. In contrast, clear SERS signals can be observed on ZIF-8 for MO (10^{-4} M) under 633 nm excitation, whereas the SERS signal of MO on the ZIF-67 sample is undetectable. These findings emphasize the importance of structural flexibility in the design of semiconducting SERS substrates and provide a high degree of variety and tailorability for SERS detection.

Organic-Inorganic Hybrid Perovskites. Inspired by the fast development of photoelectronic devices, organic-inorganic hybrid perovskites, such as methylamino lead halide perovskites ($MAPbX_3$, MA = $CH_3NH_3^+$, X = Cl^-, Br^-, or I^-), have attracted widespread attention due to their attractive optical properties and low-temperature solution synthesis. Taking $CH_3NH_3PbBr_3$ as an example, this direct-band-gap semiconductor has a large absorption coefficient, high charge-carrier mobility, and a tunable band gap over a wide range. Su and coworkers explored possible SERS applications for $CH_3NH_3PbBr_3$ crystals, with a 10^4 signal enhancement observed for 4-Mpy adsorbed on the substrate.[86] Possible EM contribution was initially excluded because single-crystal $CH_3NH_3PbBr_3$ exhibited no plasmon resonance at the excitation wavelength (633 nm). The PICT resonance was believed to be the major contributor to the observed enhancement of the SERS of $CH_3NH_3PbBr_3$ crystals, as the optical absorptions of the 4-Mpy molecule, perovskites substrate, and $CH_3NH_3PbBr_3$-Mpy complex are all non-resonant with the incident laser at 633 nm.

Conjugated Organic Semiconductors. Organic semiconductor films are promising SERS platforms for both fundamental and technological research. The utilization of π-conjugated molecular semiconductors for SERS has attracted enormous interest due to their attractive structural versatility, controllable synthesis, and film fabrication, as well as exceptional charge transport and light manipulation properties. Yilmaz and coworkers were the first to introduce organic semiconductors as candidates for SERS substrates.[87] Using an oblique-angle vapor deposition method, C8-BTBT films were fabricated with highly favorable 3D vertically aligned ribbon-like micro-/nanostructures featuring a p-type (hole-transporting) property with high charge-carrier mobility. However, the organic nanostructure obtained in this work was only used as a scaffold for a thin layer of Au (~32 nm) for SERS detection, so the observed high EF (10^8) was predominantly contributed by the plasmonic metallic layer, leaving the contributions from the molecular semiconductor undisclosed. Two years later, this same group made a breakthrough with an n-type organic semiconductor, DFH-4T, obtained via a similar vapor deposition method (Figure 6B).[88] An EF up to 3.4×10^3 for an MB probe was obtained with a DFH-4T film without the assistance of a plasmonic layer. On this substrate, EM-based Raman enhancement was ruled out considering the relatively low intrinsic carrier density (<10^{13} carrier cm^{-3}) in the DFH-4T film. Instead, a non-equivalent signal enhancement of the Raman vibrational bands suggested the dominance of CM contributions. Recently, the SERS activity of molecular semiconductors has been further improved, as observed with a fluoroarene-modified oligothiophene DFP-4T substrate. As an analog of DFH-4T, DFP-4T was constructed with a similar electron-rich quaterthiophene π-core but end-capped with π-electron-deficient perfluorophenyl ($-C_6F_5$) units.[89] A large Raman EF (>10^5) and low LOD (10^{-9} M) for an MB probe were obtained with the DFP-4T substrate comparable with those reported for inorganic semiconductors, which was similarly governed by a resonant CT between the DFP-4T film and the probe molecule.

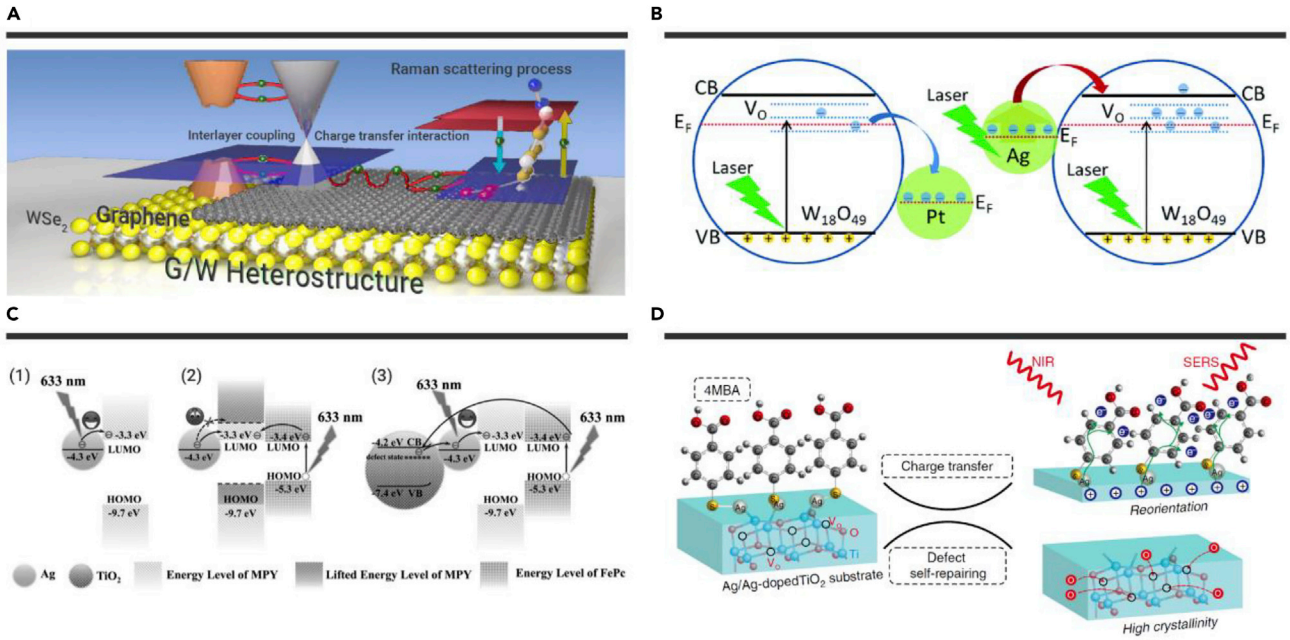

Figure 7. Van der Waals Heterostructure and Metal-Semiconductor Heterostructure. (A) Heterostructure between WSe_2 monolayer and graphene. (B) Metal/$W_{18}O_{49}$ heterojunction for controllable charge transfer. (C) Charge transfer in TiO_2-Ag-MPY-FePc System. (D) Irreversible accumulated SERS based on Ag/TiO_2 hybrid. Reprinted with permission from Tan et al.[90] (Copyright 2017, American Chemical Society) (A), Gu et al.[103] (Copyright 2018, Royal Society of Chemistry) (B), Wang et al.[104] (Copyright 2019, John Wiley & Sons, Inc.) (C), and Zhou et al.[107] (Copyright 2020, Nature Publishing Group) (D).

It is clear that the development of SERS based on organic molecules and complexes is still in its infancy, with underdeveloped candidate materials and relatively low SERS sensitivity. However, SERS substrates constructed with organic components are especially attractive for analyte-selective detection, which is regarded as a thorny problem in practical applications of SERS detection. With their almost unlimited structural molecular variations, the chemical structure of these new types of SERS substrate could be specifically tailored to optimize the capture of particular analyte molecules, as well as the formation of CT complexes in resonance with the incident laser for the molecule-substrate system.

Heterojunction with Modulated CT for Improved SERS Performance. As has been demonstrated, the SERS enhancements of semiconducting substrates are largely determined by their structural and chemical properties, and several strategies have already been widely adopted for specific categories of semiconducting substrates to enhance SERS activities, such as layer-number modulation in graphene analogs and defect engineering in metal oxides, based on CT-induced SERS enhancement. In addition to these intrinsic dominant factors, interfacial and external driving forces, such as the formation of a heterojunction, can also exert significant effects on the overall CT processes and thus alter the observed SERS effects, especially for substrates constructed with multiple components.

Van der Waals Heterostructures. A diverse range of 2D materials have their own merits with respect to both surface chemistry and electronic structures. Benefiting from an interlayer electronic tunneling effect, atomic thin-layered 2D materials held together by van der Waals (vdW) forces enable the artificial construction of the electronic band structure of the hybrid, which offers an ideal platform for the investigation of CT-induced SERS enhancement on non-plasmonic materials. The heterojunction between two semiconductors with distinct internal properties may also facilitate the unique separation of electron-hole pairs as well as increase the probability of interfacial electron transitions, leading to boosted SERS performance.

TMDs/graphene vdW heterostructures can integrate the superior light-solid interaction in TMDs with the charge mobility of graphene, and are thus promising substrates for SERS. Tan and coworkers demonstrated an enhanced Raman scattering effect based on a vdW heterostructure with large area of 10 × 10 mm^2,[90] which was constructed by stacking the WSe_2 (W) monolayer and graphene (G) in different sequences (G/W, W/G, G/W/G/W, and W/G/G/W) (Figure 7A). A stacking-sequence-dependent Raman enhancement was observed with a CuPc probe, with the G/W and G/W/G/W hybrids showing high SERS sensitivity, and the W/G and W/G/G/W substrates exhibiting intermediate SERS activities between single-component WSe_2 and the graphene monolayer. These observations confirmed previous speculations that SERS was a surficial effect and that the SERS performance in a heterostructure was highly dependent on the uppermost material layer, which would increase upon the interfacial CT within the heterostructure. In addition to the improved CT contribution, other resonance effects such as exciton and plasmonic resonances could also be facilitated in such heterostructures. With the TMD (MoS_2 and WS_2) nanodome/graphene vdW heterostructure reported by Ghopry and coworkers,[91] a significantly improved SERS sensitivity for R6G was observed at resonant Raman excitation (532 nm), exceeding that on single-layer TMD and graphene substrates by more than three orders of magnitude. In addition to the enhanced CT at the interfaces of the TMD/graphene vdW hybrid, the authors also suggested a possible LSPR contribution provided by discrete TMD nanodomes on the graphene layer. In another example, the SERS sensitivity of a graphene/ReO_xS_y vertical heterostructure was optimized by controlling the lattice oxygen concentration of ReO_xS_y during solution-phase growth, in which an LOD of 10^{-15} M was obtained for the R6G probe.[92] An oxygen-induced band-level alignment of the CT resonance and dipole-dipole interactions with the probe molecules were both believed to be responsible for the SERS activity. More importantly, further magnified PICT and exciton resonances in ReO_xS_y were believed to be induced by the heterostructure through an interlayer coupling effect, which also contributed to the SERS effect.

Beyond graphene, vdW heterostructures can also be constructed between layered TMDs or even other semiconductor nanoparticles, with new insights proposed for the mechanism of SERS enhancement based on the CT and energy transfer across the atomic-scale interfaces. Li et al. obtained a vertical heterojunction between $W_{18}O_{49}$ and monolayer MoS_2, in which a tungsten oxide layer was magnetically sputtered onto CVD-derived MoS_2 followed by reduction in an H_2 atmosphere.[93] Enhanced Raman scattering was observed with the semiconductor heterojunction, with an EF of 3.45 × 10^7 and an LOD of 10^{-9} M for an R6G analyte. The dramatically enhanced

PICT processes in the heterojunction were believed to responsible for the SERS, based on the promoted charge-carrier separation and exciton resonance induced by the heterojunctions. As an interesting example reported by Hu and coworkers,[94] few-layered black phosphorus (BP) quantum dots (QDs) were utilized to construct vdW heterojunctions with a ZnO nanorod. In the hybrid, the degree and even direction of the CT could be modulated by adjusting the indium content in the ZnO nanorod, leading to mutual enhancements in Raman scattering between ZnO and BP. By tracking the Raman bands of BP or ZnO as internal probes at 514.5 nm excitation, the EF values of the ZnO nanorod and BP QDs in the hybrid were calculated to be 121 and 4,340, respectively. Furthermore, the SERS enhancement for the two inorganic probes was explained by the CM attributed to the PICT contribution, dipole interactions, and assembly configuration of the disk-shaped BP QDs on ZnO surface.

In addition to the EM and CM contributions discussed above, the relatively weak interactions (relative to those of chemical bonding) between two semiconducting components in a vdW heterostructure may also facilitate the SERS enhancement with additional contributions. Recently, with a vertical vdW heterostructure comprising a monolayer MoS_2 placed on a multilayer $SnSe_2$, Dandu and coworkers demonstrated Raman enhancement driven by non-radiative energy transfer (NRET) as a novel mechanism, achieving a 10-fold enhancement in total Raman intensity.[95] As NRET is determined by the spectral overlap of the donor emission and the acceptor absorption, the contribution from NRET was determined based on a strong modulation in the EFs by tuning the spectral overlap between MoS_2 and $SnSe_2$. As the NRET arose from long-range Coulomb interaction, it was validated by introducing an h-BN spacer (10-nm thick) between MoS_2 and $SnSe_2$ to block possible direct CT while allowing Coulomb interaction. As expected, a lowered Raman intensity was observed from MoS_2/hBN/$SnSe_2$ relative to that of MoS_2/$SnSe_2$, suggesting the reduced efficiency of NRET upon spatial separation in the heterojunction and further confirming the NRET contribution to SERS.

Metal-Semiconductor Heterojunctions. The heterojunctions between metals (e.g., Au, Ag) and semiconductors cover a broad spectrum of active SERS substrates, as discussed in detail in several published reviews.[13,17,96] Benefiting from the EM of the metal components, metal-semiconductor heterojunctions as SERS substrates typically show EF values orders of magnitude larger than the single semiconductor component. More interestingly, the modulated CT across metal-semiconductor interfaces may promote a deeper understanding of the SERS mechanism and broaden the applications of such hybrid substrates.

Graphene has long been recognized as a desirable platform in combination with noble metals due to its atom-level flat surface. A graphene-mediated SERS (G-SERS) substrate was fabricated by Xu and coworkers,[97] with Au/Ag nanoislands (8 nm in height with 2- to 3-nm gap) tightly adhered on the back of a monolayer of graphene. By collecting electromagnetic hot spots created by LSPR from the side of graphene, the G-SERS substrate was expected to provide an atomically smooth surface for reproducible Raman signals, controllable molecular arrangements, and well-defined molecular-substrate interactions. In another example,[98] r-GO nanosheets decorated with Ag nanoparticles showed sensitivity toward the SERS detection of aqueous uranyl (UO_2^{2+}) ions with an LOD as low as 10 nM. In this hybrid, r-GO serves as a scaffold that promotes the generation of a plasmonic Ag hot spot as well as the adsorption of uranyl species, and the CT effect was found to be responsible for the SERS enhancement, as indicated by the spectral shift of the symmetric stretching mode of UO_2^{2+} ions. Multifunctionality can also characterize SERS substrates based on a rational design of the metal-semiconductor heterojunction, as demonstrated by Qu and coworkers[99] using Au nanoparticles with a diameter of 30 nm modified on the surface of g-C_3N_4/GO nanosheets. By combining improved SERS sensitivity with photocatalytic activity, this hybrid was used as a membrane and demonstrated multifunctional merits, including pre-concentration capability, SERS identification, SERS removal, and the recyclable SERS detection of 4-chlorophenol. Beyond graphene, MXenes as SERS substrates show certain advantages, including ease of manufacture, strong LSPR arising from abundant free electrons, and facilitated CT due to the variety of surface sites. Yu et al. proposed a new MXene/Au heterostructure in which $Ti_3C_2T_x$ (T_x indicating the surface functional groups of −OH, −F, −O) nanosheets were deposited on self-assembled Au nanostructures via a layer-by-layer spin-coating method.[100] Benefiting from a magnified electromagnetic field by the underlying Au component, the MXene/Au architecture showed a high EF value of 2.9×10^7 for R6G at a low concentration (10^{-10} M). The authors suggested that the MXene upper layer contributed in a number of respects, including the prolongation of the enhanced EM field distribution, contribution of an additional electron for the molecular vibration, and protection of the analyte from denaturation upon direct interaction with Au NSs.

In addition to the decoration of noble metal nanoparticles on a planar semiconductor discussed above, diverse metal-semiconductor heterogeneous nanostructures have also been developed and shown to have improved SERS activity. Colloid-synthesized matchstick-shaped Au-ZnO heterogeneous nanorods were developed by Zhou et al. via facile one-pot colloid synthesis.[101] The hybrid featured a Zn-ion terminated plane at the ZnO-Au interface without the formation of Au−O bonds, as evidenced by the atomic-resolution observation of the interfacial structure and electronic states. When dopamine, a molecule tightly bound to the surface of ZnO with a large CT, was chosen as an SERS probe, further improved SERS sensitivity was observed on the hybrid with respect to Au seeds alone, which was experimentally ascribed to the CT contribution and LSPR-enhanced CT effect in the hybrid. Among the numerous non-planar heterogeneous nanostructures, plasmonic nanostructures with a core@shell geometry are especially attractive as they offer controllable overlap between the enhanced electric field and the semiconductor shell, thus further protecting the metal core from undesired surface interactions. In fact, SERS substrates based on the core@shell heterostructure have already been developed as an important branch of study in SERS, showing potential in both applications and CT mechanism investigations. O'Neill and coworkers demonstrated an example of Ag@CeO_2 nanocubes as an effective SERS substrate,[102] in which a 4-MBA linker between core and shell was used as a probe for monitoring the PICT transitions by Raman spectroscopy. By comparing the intensities of totally symmetric and non-totally symmetric modes, the degree of PICT was found to increase with decreasing excitation wavelength, which could be fully explained by a direct CT transition from the Ag Fermi level to the LUMO of 4-MBA. Additionally, an increase in the CT yield was found with increasing ceria shell thickness, which was ascribed to the relaxation of excited electrons further into the ceria CB, accompanied by the formation of oxygen vacancies. These results provide a deeper understanding of PICT in metal-semiconductor heterostructures.

Due to the typically large discrepancy in the work functions of noble metals and semiconductors, band-level alignment may widely exist at the metal-semiconductor conjunction. In fact, the CT across metal-semiconductor interfaces can be modulated in their efficiencies and even direction, based on the Schottky barrier and LSPR effect introduced by the metal component. Therefore, aside from the EM contribution by the metal component, such an interfacial CT may significantly affect the intrinsic SERS enhancement of the semiconductor component. To verify this speculation, Gu and coworkers compared the SERS performances of Ag-$W_{18}O_{49}$, Pt-$W_{18}O_4$, and pristine $W_{18}O_{49}$ samples, with the Ag/Pt loading amount at a similar ratio (around 1 wt %) for the two hybrid samples (Figure 7B).[103] Distinct EFs with the trend sequenced as Ag-$W_{18}O_{49}$ > $W_{18}O_{49}$ > Pt-$W_{18}O_{49}$ were obtained for an R6G analyte on the three substrates. Clearly, the SERS effect of the $W_{18}O_{49}$ substrate was able to be modified when decorated with noble metals, being enhanced when using Ag as a loading component but impaired when using Pt. After excluding the possible EM contribution in control experiments, a CT-induced charge accumulation on the semiconductor component was inferred to be the main reason for the enhanced SERS. To obtain a detailed picture of the electron flow at metal-semiconductor interfaces, the interfacial CT between the noble metal and semiconductor was taken into consideration, which can make a great change in the carrier intensity at the surfaces of semiconductors through two opposite pathways. In the dark, when an Ag (E_F = −4.49 eV) or Pt (E_F = −4.26 eV) metal is in physical contact with $W_{18}O_{49}$

(E_F = −5.65 eV), electrons will flow between $W_{18}O_{49}$ and the metal, with a Schottky barrier formed at the equilibrium. Inversely, under illumination at the SPR frequency of noble metals, "hot electrons" will transfer from the metal nanoparticles to the CB and trapped states (e.g., oxygen-deficit states V_O) of the semiconductor, opposing the Schottky barrier's natural tendency. As a result, the visible plasmonic Ag would facilitate electron accumulation in $W_{18}O_{49}$, whereas Pt as an electron sink would decrease the electron population of $W_{18}O_{49}$ in contact. This electron-accumulation-induced SERS effect in semiconductors was also verified by a donor-acceptor-type interaction with organic molecules. When $W_{18}O_{49}$ alone was used as an SERS substrate, a significant enhancement in the signal intensities of an R6G analyte could be observed with the presence of a trace amount of ATP, due to its chemical bonding to $W_{18}O_{49}$ with an electron-donating effect. Similarly, an altered direction of the interfacial CT in a TiO_2-Ag-Mpy-FePc system was also demonstrated in detail by Wang and coworkers, as revealed by SERS (Figure 7C).[104] Upon the stepwise introduction of FePc (iron phthalocyanine) and TiO_2 components to an initial Mpy-modified Ag substrate, PICT from Ag nanoparticles to Mpy was inhibited by FePc while being further promoted by TiO_2, as evidenced by the selective enhancements in the a_1 and b_2 modes, respectively. The inhibition by FePc was ascribed to the FePc-Mpy coordination, leading to an increased energy gap between the Fermi level of the Ag nanoparticles and LUMO level of Mpy. In contrast, the further promotion by TiO_2 was due to the "bridge" effect of TiO_2 in contact with both FePc and Ag, for a fluent CT mediated from photosensitized FePc to Ag nanoparticles.

Based on the dynamically controlled CT across the interfaces of the metal-semiconductor heterojunction, photoinduced-enhanced Raman spectroscopy (PIERS) was proposed by Ben-Jaber and coworkers,[105] with a hybrid fabricated by decorating Au (27 nm) or Ag (58 nm) onto CVD-derived TiO_2 rutile (R) film. This effect was essentially an activation of the TiO_2 substrate via pre-irradiation, based on UV-light-mediated electron migration from the semiconductor substrate to the metallic nanoparticle, accompanied by the creation of V_O defects on the TiO_2 surfaces. Then, with Raman laser excitation, electrons would be promoted from V_O states into the CB of TiO_2 followed by a transfer into Au energy levels, leading to increased sensitivity an order of magnitude beyond normal electromagnetic SERS. The essential operation of this enhancement was suggested to be related to the modification of the Fermi level of the metallic nanoparticles with broadened resonance conditions between the Fermi level and molecular orbitals to facilitate CT transitions, thus being applicable to a wider variety of molecules with low Raman cross-sections, such as pentaerythritol tetranitrate, cyclotrimethylenetrinitramine, and glucose, as well as the vapor-phase detection of TNT (7 ppb). However, due to the surface healing of the defect upon exposure to air, an intensity decrease in the PIERS signal is inevitable within the initial 30–60 min after pre-irradiation of the substrate. Al-Shammari et al. extended this strategy to a lithium niobate film substrate decorated with photodeposited Ag nanoparticles, which showed a 7-fold increase in the signal intensity of ATP.[106] The enhancement from PIERS was demonstrated to last for a time span of ~10 h, which is an order of magnitude longer than that observed with the previously reported TiO_2-based substrate. The PICT from the substrate to 4-ABT was confirmed to be the main contribution to the observed enhancement, with a relatively slow charge recombination rate in lithium niobate being responsible for the increased PIERS duration. In essence, the PIERS effect observed with metal-semiconductor hybrids is related to the creation of oxygen vacancies in the excited semiconductor component, relying on pre-activation by high-energy UV photons. Altered SERS activities have also been observed on similar metal-semiconductor hybrids but by near-infrared (NIR) irradiation. An interesting irreversible accumulated SERS behavior was reported by Zhou and coworkers with an Ag/Ag-doped TiO_2 hybrid nanostructure, induced by prolonged 785-nm laser irradiation (Figure 7D).[107] By simultaneously monitoring the characteristic Raman signals of both the 4-MBA analyte and TiO_2 substrate, a time-dependent SERS behavior was observed with continuous 785-nm irradiation, whereby an irreversible increase and decrease was obtained in the signal intensities for 4-MBA and TiO_2, respectively. The time-dependent SERS behavior upon NIR irradiation was explained by several factors, including the improved crystallinity of the Ag/Ag-doped TiO_2 substrate, the PICT effect, and a charge-induced molecular reorientation. These interesting irradiation-dependent SERS behaviors of the metal-semiconductor hybrid are closely related to the CT transitions, which enable a better understanding of CT-induced SERS enhancements.

Interfacial Chemical Bonding in and External Stimulations to Substrates with CT-Based Enhancement. Interfacial Chemical Bonding. Distinct from the remote field enhancement by EM, CT-based CM contribute to the SERS signals only if the analyte binds directly with the substrate surface. Thus, CM enhancements to SERS are closely associated with the interfacial bonding between the molecule and substrate, ranging from weak physical adsorption, moderate electrostatic interaction, and hydrogen bonding to the formation of a CT complex or strong covalent bonds.

SERS probes selected for noble metals (Au, Ag) usually feature N- or S-based functional groups, partially due to their strong affinity to metals by covalent bonding. For instance, dibenzothiophene (DBT) is a typical S-containing heterocyclic compound recognized as a pollutant in liquid fuels, which has its optical absorption in the UV region, far from overlapping with the plasmonic band of Ag (400 nm) or Au (500 nm), and thus is practically "invisible" for SERS. To achieve resonant Raman scattering enhancement for these important analytes, Sidorov et al. proposed a strategy for entrapping these compounds into CT complexes, which would then be immobilized onto nanostructured Ag substrates.[108] A colored donor-acceptor CT complex would be formed between the electron-rich DBT and 2,3-dichloro-5,6-dicyano-1,4-benzoquinone as a π electron acceptor, leading to improved sensitivity in SERS and surface enhanced resonance Raman spectroscopy analysis.

As another important interfacial interaction, hydrogen bonding is a dipole-dipole interaction with relatively weak bond strengths (1–9 kcal/mol); however, it can significantly affect the CT-induced SERS enhancement due to its short-range (0.25–0.35 nm) effect. Wang and coworkers explored the effect of intermolecular H bonding on the CT contributions to SERS.[109] 4-MBA molecules as an SERS probe were pre-adsorbed onto an Ag nanoparticle assembly by the formation of Au–S bonds, and soaked in aniline with different concentrations before in-solution SERS measurement. Both the intensities and vibrational frequencies of certain characteristic peaks for 4-MBA were found to be associated with the H-bond formation between 4-MBA and aniline molecules, and the dramatically enhanced non-totally symmetric (b_2) mode of MBA was used as a manifestation of the CT transition process in this system.

External Stimulations. External stimulations from the surrounding environment, such as the pressure, electrochemical potentials, and pH values of the solution, will also alter the electronic properties of both metal and semiconductor substrates, which enables modulation of the CT processes for enhanced SERS effects.

Since the discovery of the SERS effect on a rough Ag electrode, electrically modulated SERS (E-SERS) has been widely used and is predicted to have the capability to realize a 10-fold enhancement in the overall SERS signals via modulable Fermi levels and the plasmonic resonance of metallic nanostructures. However, electronic modulations in electrode materials have often been performed in electrolyte solutions, which necessitate an electrochemical cell set. To address the inconveniences of E-SERS, Li et al. developed a self-energizing E-SERS substrate fabricated with plasmonic Ag nanowires and a piezoelectric polymer, PVDF-HFP, separated by polyethyleneimine/r-GO as filler.[110] By the pressing of a finger, piezoelectric voltages were generated on the deformed substrate to generate a prolonged (tens of seconds) negative potential that caused electron flow into the Ag nanowires with enhanced SERS intensity. CM and EM were suggested to both contribute to the charged state of the substrate, as evidenced by the experimental observation of peak splitting and frequency shifts in the Raman spectrum, and the simulation results for the magnified electrical field in the Ag nanowires.

In comparison with metals, CT-induced chemical enhancements exhibit a rather close relationship with the external stimulations of semiconductor substrates, as the energy-band structure of the semiconductors can be

0effectively modulated by stimuli such as changes in the chemical environment or pressure. For instance, the band-edge position of TiO_2 is sensitive to pH, showing a negative shift in the CB edge along with the increasing pH of the solution, which can increase the electron density in the CB in an equilibrium state. Based on this pH-mediated band-structure modulation in TiO_2, the observed variation with pH of the SERS signals of Ag/4-mercaptophenol/TiO_2 would be explained by the CT contributions.[111] Pressure is also demonstrated to affect the degree of CT in TiO_2, due to the pressure-induced reduction in the E_g of the TiO_2 nanoparticles. For example, a high-pressure-induced blue shift and change in the intensity of the Raman spectra of 4-MBA@TiO_2 solid powders has been reported, with the degree of CT reaching a maximum at a pressure of 4.40 GPa.[112] Similar pressure-induced SERS enhancement was also found in a MoS_2/Au/R6G hybrid, based on the pressure-manipulated band alignment of the molecule and substrate. Using this strategy, the authors reported an optimized Raman enhancement for R6G molecules with MoS_2/Au substrate at 2.39 GPa, with a maximum degree of charge transfer (ρ_{CT}) achieved between the R6G molecule and MoS_2/Au substrate.

Based on rationally designed interfaces and suitable external stimulations, the efficiencies and pathways of CT transitions in the molecule-substrate system can be effectively modulated to further improve SERS sensitivities. Moreover, with the Raman signals indicative of the CT contributions, interfacial interactions between molecules and substrates can be revealed, which promises wider application of SERS beyond traditional analytical detection.

Applications of SERS in Terms of Interfacial CT Process

SERS spectra can provide fingerprint information about a target molecule accompanied by alteration of its spectral features, such as band positions and relative intensities, when the probe molecule is chemically bonded to the surface of a substrate. Thus, in addition to their development as sensors for trace analysis, novel applications of SERS substrates have been exploited in terms of interfacial CT processes. For instance, the interfacial interactions between molecule and substrate can be determined, including the surface bonding, orientation, and conformation of the adsorbed molecules. Additionally, *in situ* monitoring of interfacial processes can also be realized, ranging from catalytic reactions and surface structural changes to charge/discharge in batteries, to name a few.

Sensors for Environmental and Health Analysis. Trace analysis, a major topic in SERS research, has already been developed as an efficient protocol for practical applications, such as the detection of harmful residues in food and environmental specimens. In such practical systems with complex compositions, the sensitivity of the SERS substrate is no longer the only criterion of interest, as it is often of equal importance to reduce spectral interference from components of no interest or even realize the selective enhancement of target molecules. He and coworkers have made systematic progress in the development of a methodology for SERS detection in practical systems, based on the construction of nanostructured plasmonic SERS sensors. First, they developed a method for identifying the geographic origins of *Coptis chinensis* using SERS that does not require strict separation and complex pre-processing.[113] They then used a novel strategy that combined iterative cubic-spline-fitting baseline correction with discriminant partial least-squares qualitative analysis to analyze the SERS spectra of banned food additives, such as Sudan I dye and RhB, and Malachite green residues in aquaculture fish, based on an Au-plated silicon SERS substrate.[114] Furthermore, they designed a trans-scale bimetallic substrate fabricated with a vacuum-deposited Ag island film on Au-film inverted pyramid pits (2-mm period) for the detection of BPA at an LOD of 0.5 ppm.[115] Recently, by using a ratiometric SERS aptasensor based on internal standard (IS) methods, two simple and accurate assays constructed with plasmonic core-shell nanostructures have been developed for the sensitive detection of certain important practical species in the environmental and food fields, such as ochratoxin A and microcystin-LR.[116,117] 4-ATP molecules and GO/Fe_3O_4 nanoparticles showing a stable Raman band were used as internal standards in the two SERS assays, respectively. With correction by the IS Raman signals, quantitative detection of the target molecule was realized by SERS. Therefore, the protocol provides a reliable and rapid method for the sensitive and quantitative detection of various molecules and exhibits excellent application prospects in complex systems.

In addition to the detection of target molecules in food and the environment, the identification of biomarkers related to *in vivo* cells is another challenge for SERS. The analysis of volatile organic compounds (VOCs) with SERS is an attractive strategy for the rapid screening of diseases, e.g., the aldehydes in human exhaled breath have been used as indicators of lung cancer. However, the weak Raman scattering and low affinity of gaseous molecules on SERS substrates are two major obstacles for VOC-based diagnostics. Qiao and coworkers used an Au@ZIF-8 3D structure constructed by coating a ZIF-8 layer onto self-assembled gold superparticles (GSPs) for the SERS detection of gaseous aldehydes (Figure 8A).[118] Via the porous structure of the MOF shell, gaseous aldehydes released from tumor-specific tissue could be channeled onto an SERS-active GSPs core through the inherent interstices of the ZIF-8 shell and then be captured by pre-grafted 4-4-ATP molecules via a Schiff base reaction for detection at the parts-per-billion level. Their study involved the selective detection of a trace gaseous cancer biomarker in a multicomponent gas on a metal-semiconductor hybrid, thus demonstrating the potential of SERS in real-world applications.

Recently, femtosecond pulsed laser ablation was used by Ganesh and coworkers in the synthesis of quantum-sized semiconducting nanostructures, which showed significant sensitivity toward various cancerous biomarkers. For instance, a quantum-sized organic semiconductor (QOS) nanostructure was obtained by ionizing graphite by femtosecond pulsed laser ablation, which exhibited a high EF of 10^{12} for R6G.[119] To detect single-molecule genomic DNA, a QOS was used as a tag-free SERS sensor for the identification of a cancer stem cell phenotype by isolating genomic DNA from various cell lines, including fibroblast cells (NIH3T3), breast cancer (MDA-MB 231), pancreatic cancer (AsPc-1), and lung cancer (H69-AR). In another example, femtosecond pulsed laser treatment was applied to the synthesis of quantum-scaled ZnO, which was then combined with a nanodendrite platform for cell adhesion, proliferation, and label-free detection.[120] By analyzing the rated peak intensities for lipids and proteins (I_{1445}/I_{1654}), *in vitro* discrimination between cancer and non-cancer cells was realized by SERS. The observed SERS performance was ascribed to the pulsed-laser deposited ZnO with a high carrier density and oxygen vacancies, facilitating the combined resonant contributions of the PICT, exciton, and plasmon resonances. Additionally, an SERS platform with multiple functions for the simultaneous diagnosis and treatment of cancer cells was reported by Lin and coworkers,[121] who developed black TiO_2 nanoparticles featuring a crystal-amorphous core-shell structure obtained by solid-state synthesis. The as-prepared B-TiO_2-based SERS bioprobe simultaneously obtained SERS sensitivity and a photothermal therapeutic effect toward MCF-7 drug-resistant breast cancer cells, which was ascribed to the heterojunction between the crystal and amorphous components, efficient exciton separation at the interfaces, and the high electronic DOS in the amorphous shell of the heterostructure.

Chirality is an inherent feature of biological systems, and chiral discrimination has become a fundamental feature of living organisms that is also attractive in the field of catalysis and synthesis. Because CT-induced SERS is sensitive to variations in the molecular environment, e.g., intermolecular hydrogen bonding, variations in the SERS spectrum can be expected for a chiral selector placed in distinct chiral environments. Using Ag nanoparticles modified with 4-Mpy as a chiral selector, Wang and coworkers were the first to demonstrate the enantioselective discrimination of alcohols (1,1,1-trifluoro-2-propanol) by SERS, with the enantiomeric excess (*ee*) value determined by the ratio of the relative intensities of bands near 1,200 cm^{-1}.[122] The spectral discrepancy was ascribed to the formation of intermolecular hydrogen-bonding complexes of alcohols with different molecular orientations in the presence of a chiral selector, thus leading to different CT states and relative intensities among the vibrational modes. Based on this chiral, "label-free" discrimination mechanism, the authors enlarged the sensitivity and scope of the enantiomeric recognition by constructing Ag-TiO_2-Ag

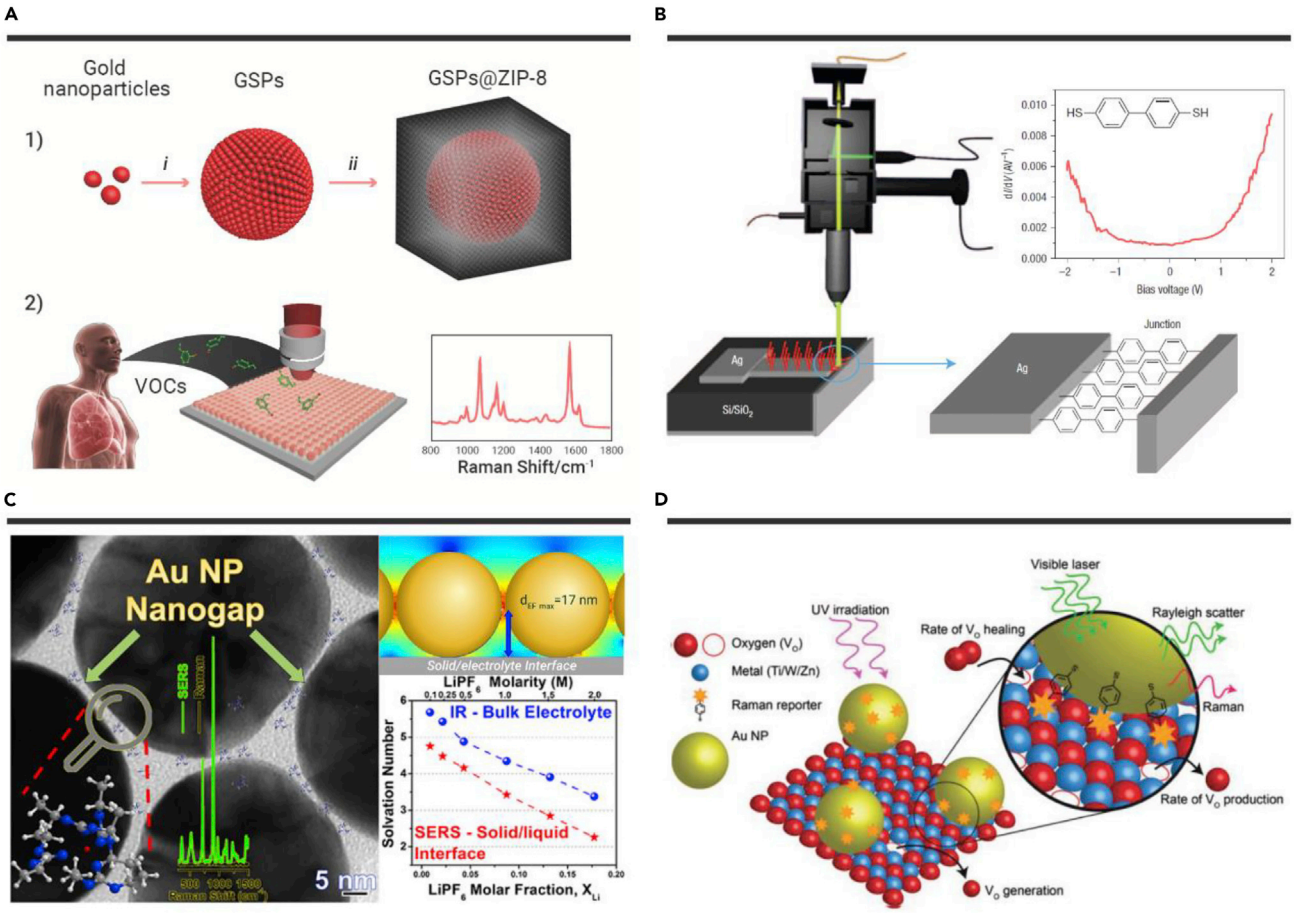

Figure 8. Typical Applications of SERS (A) Au@ZIF-8 3D structure for cancer-related VOCs diagnostic. (B) Scheme of an "on-edge" junction under Raman setup. (C) SERS detection of the electrolyte solvation structure at solid-liquid interface. (D) SERS monitoring the dynamics of photoinduced surface oxygen vacancies in metal-oxide semiconductors. Reprinted with permission from Qiao et al.[118] (Copyright 2018, John Wiley & Sons, Inc.) (A), Ioffe et al.[130] (Copyright 2008, Nature Publishing Group) (B), Yang et al.[132] (Copyright 2018, American Chemical Society) (C), and Glass et al.[133] (Copyright 2019, John Wiley & Sons, Inc.) (D).

sandwich substrates consecutively modified by monomers of (6-mercapto-6-deoxy)-β-cyclodextrin and 4-ATP as the stereo-selective capture component and chiral selector, respectively.[123] They then demonstrated a sensitive discrimination response to different L-amino acid enantiomers with respect to D-amino acids by the enantioselective sensor. These results contribute to the field of label-free enantioselective discrimination by means of SERS platforms, in which the contributions from the CT are emphasized.

Catalytic Reaction Monitoring. Catalytic reactions over a solid catalyst are usually accompanied by an interfacial CT, which is one of the core issues in determining the exact reaction path needed to improve catalytic performance. Sharing the same CT pathways, SERS can be used as an effective analytical means for the *in situ* monitoring of reactions catalyzed exactly by the SERS substrates.

Plasmonic metal-based nanostructures can cause redistribution not only of the electromagnetic fields but also the excited carriers (electrons and holes) under excitation, and have been widely exploited as bifunctional platforms that exhibit both SERS and catalytic activities. De Nijs et al. fabricated a self-assembled nanoparticle-on-mirror Au geometry that featured small gap separations between Au nanoparticles and the underlying atomically smooth Au substrates, as directed by the molecular size in the self-assembled monolayer.[124] The molecular spacers were found to act as molecular tunneling junctions at the nanoscale, providing low-energy tunneling pathways for the movement of excited charge carriers between metal surfaces. With this structural design, hot-electron-induced chemical reduction processes in aromatic molecules (e.g., bipyridine analogs) were able to be tracked by SERS. A detailed introduction to the *in situ* study of plasmon-mediated chemical reactions by SERS can be found in an article by Zhan et al.[125] By taking the plasmon-mediated transformation of 4-ATP as a typical reaction, the authors described a method for identifying changes in SERS spectra induced either by surface reactions or chemical enhancement, and further proved that the selective transformation of 4-ATP would be either via hot-electron-induced oxygen activation or oxidation by hot holes in the absence of oxygen. In both cases, the interfacial CT transitions between the reactants and plasmonic nanostructures were core contributions.

The oxygen reduction reaction (ORR) is one of the fundamental reactions in fuel cells. Based on the SERS effect by Au@SiO_2 shell-isolated nanoparticles (SHINs), Dong and coworkers used SHINs as an *in situ* reporter of the ORR process on Pt(hkl) single-crystal surfaces.[126] With about 30% coverage of SHINs on the surface of the Pt(hkl) electrode, Raman signals of active oxygen species such as OH*, HO_2*, and O_2^- involved in an ORR process could be obtained as direct spectral evidence of the catalytic reaction. Hybrid electrocatalysts that combine metals and semiconductors are usually designed for improved catalytic efficiencies by charge-carrier separations, whereby the CT pathways can also be monitored by SERS. Electrocatalytic water splitting has also attracted great attention due to its environmentally friendly energy production. The oxygen evolution reaction (OER) and hydrogen evolution reaction (HER) are two half-reactions in the electrocatalytic water-splitting process, both of which are critically influenced by the catalyst surface sites and the CT transitions across interfaces. Du et al. prepared Au-decorated Ni-Co-layered double hydroxide (NiCo LDH) as a plasmonic electrocatalyst for water splitting with the assistance of visible irradiation.[127] To determine the reaction pathways in the as-prepared

catalyst, 2,6-dimethylphenyl isocyanide was used as an SERS probe to examine the CT processes in the hybrid due to its covalent bonding to metal (Au nanoparticles) and the varied strength of the N≡C bond as affected by the electron abundance of the metal. According to the spectral evidence obtained by SERS, a spontaneous interfacial CT from NiCo LDH to Au was found, which facilitates both the OERs and HERs. Using SERS detection, the authors verified that HER and OER mainly occurred on the surface of plasmonic Au and semiconducting NiCo LDH, respectively.

Interface Process Tracking. Interfacial chemistry is at the core of optoelectronic applications for both metals and semiconductors; however, direct tracking of the interfacial processes is difficult due to their transient dynamics. As an *in situ* analytical method with high resolution that is applicable in aqueous environments, SERS has shown unique feasibility for the monitoring of certain interfacial processes, such as CT, interfacial properties, and even local heating.

Wang and coworkers conducted a systematic investigation of interfacial CT processes tracked using the SERS technique, based on the rational construction of metal-semiconductor heterostructures with the probe molecule as a linker at the interfaces. With this sandwich system design, the SERS technique was demonstrated to be an attractive means for monitoring interfacial CT behaviors in hybrids, which is especially in demand by the development of modern photovoltaic devices. For instance, with the demonstration of a solar cell-like TiO_2-Ag-Mpy-FePc system, the photoelectric performance of the interfacial material was evaluated by SERS in a photovoltaic device.[104] Similarly, the chemical binding types and CT processes, which are critical in dye-sensitized solar cells, were determined by the construction of metal-dye-semiconductor sandwich structures, such as Ag/N719/TiO_2 and Au@Ag/N3/n-TiO_2 systems.[128,129] These strategies broaden the scope of SERS applications and make the *in situ* tracking of the interfacial CT transitions realizable.

The stability and performance of nanoscale electronic devices are significantly influenced by the local heating effect, especially at current-carrying molecular junctions with low heat capacity. Because the effective temperature at the molecular junction is related to the inelastic scattering of electrons and can be reflected by molecular vibrations, SERS can be a spectroscopic tool for heat monitoring, based on the non-equilibrium occupancy of the vibrational modes. Ioffe and coworkers demonstrated this concept using a delicate design with a self-assembled monolayer of 4,4′-biphenyldithiol molecules as linkers for two adjacent sides of an "on-edge" Ag nanostructure (Figure 8B).[130] By recording the ratio of anti-Stokes to Stokes lines in the Raman vibrational mode, they obtained the mode-specific effective temperature at the molecular junction.

The interfacial hot-electron transfer directly determines the efficiency of plasmon-mediated photocatalysis, which can be monitored based on bifunctional configurations that allow both photocatalysis and *in situ* SERS effects. The interfacial hot-electron transfer behavior identified by SERS was first developed by Zhang and coworkers[131] in a comparative study of different core@shell heterostructures, in which Au cores were coated with SiO_2, TiO_2/Cu_2O, and Pd/Pt as the insulator, semiconductor, and metal, respectively. Based on the changes in Raman signals of the 4-ATP and *p,p*′-dimercaptoazobenzene during photocatalytic conversion, the authors concluded that hot electrons would transfer across the Au-semiconductor and Au-metal interfaces but be blocked at the Au-insulator interface, with the migration distance more than 10 nm in semiconductors but less than 1 nm in metals. This work demonstrates the possibility for *in situ* monitoring of the interface process with the assistance of a suitable SERS substrate.

Charge transport at the electrode-electrolyte interfaces, one of the rate-limiting steps of battery charge/discharge, is critically determined by reversible ion solvation and desolvation processes. However, the characterization of the electrolyte solvation structure under *in operando* conditions remains a big challenge. Yang and coworkers reported an SERS detection of the electrolyte solvation structure at the solid-liquid interface based on a sealed transparent Raman cell configuration, in which a monolayer of Au nanoparticles (36.7 ± 2.8 nm) self-assembled on a Ni current collector was enclosed as the plasmonic SERS substrate (Figure 8C).[132] By magnifying the electromagnetic field in the gap region of the substrate, a 10^5 enhancement in Raman signals was obtained for electrolyte components such as lithium hexafluorophosphate, fluoroethylene carbonate, ethylene carbonate, and diethyl carbonate. This SERS-based spectroscopic approach was suggested to be capable of probing the Li^+ salt solvation structures in an aprotic solution within ~20 nm of the solid electrode-liquid interface.

Apart from interfacial processes associated with mass, charge, and energy transport, surface structural changes in the substrate itself can also be monitored by SERS. Glass et al. reported a PIERS effect observed in a plasmonic metal-semiconductor hybrid, with the enhancement based on the surface oxygen vacancies (V_O) that formed on semiconductor surface pre-irradiated with high-energy photons. Conversely, such a chemical enhancement in SERS enables the estimation of atomic V_O dynamics in the surface region of metal oxides (Figure 8D).[133] By combining MBA-functionalized Au nanoparticles with different semiconductors, i.e., TiO_2, WO_3, and ZnO, the formation and healing rates of surface V_O in semiconductors could be monitored by SERS under *in operando* conditions, as reflected by the Raman signal intensities of the MBA probe. Although these observations were based on an indirect measure of the effective changes in the induced oxygen vacancies, the results still indicate a potential application of SERS for *in situ* structural monitoring on metal oxide surfaces.

Challenges and Perspectives

Since its discovery, the past half century has witnessed the growth of the SERS technique, which is mainly based on plasmonic metals. In contrast, non-metal materials as promising SERS substrates have been introduced in recent decades, with further advances and developments in the past five years. Today, ever-increasing SERS activity is documented in a variety of semiconducting material categories, ranging from graphene, TMDs, and transition-metal oxides to MOFs and conjugated molecules, which generally feature CT-induced enhancement as the prominent contributor to the SERS effect. In contrast to plasmonic metal substrates that emphasize nanostructures for the generation of electromagnetic hot spots, strategies based on the regulation of chemical configurations, such as defect engineering and surficial functionality, have become central to boosting the SERS activities of these semiconducting substrates, which exhibit SERS sensitivities approaching those of their metal counterparts. Meanwhile, with the SERS enhancement induced by CT across the substrate-molecule interface, new phenomena that offer deep insight into the surficial/interfacial processes have been achieved with these semiconducting materials, greatly broadening the applicable scope of the SERS technique. Overall, SERS based on CT-induced enhancement provides new opportunities for the incorporation of non-metal materials as SERS substrates. These materials show fantastic potential to supplement the well-developed plasmonic metal substrates. Although progress has been steady, SERS based on these non-metal materials is still in its infancy, with many challenges to solve for their future development. (1) The SERS sensitivity is still insufficient to meet the requirements of practical detection applications, which can be improved by combining multiple CT transitions based on energy-level matching in the molecule-substrate system measured under resonant excitation. (2) In comparison with SERS sensitivity, signal reproducibility has often been overlooked in studies of semiconducting substrates, especially when processing powder samples. Processing substrates with uniform surficial morphologies and precisely controlled chemical compositions should be emphasized for reproducible SERS detection in these non-metal substrates. (3) In view of the CT-induced SERS enhancement, the selective detection of target molecules in multicomponent specimens is in extreme demand for practical SERS applications, and semiconducting materials can be used as ideal substrates due to their adjustable band structure and surface chemical configurations. (4) SERS enhancements in semiconducting materials are usually based on the CT being relevant to their optoelectronic functionalities, which makes SERS an ideal *in situ* characterization technique for tracking interfacial processes of general concern in catalysis and energy storage.

REFERENCES

1. Fleischmann, M., Hendra, P.J., and McQuillan, A.J. (1974). Raman spectra of pyridine adsorbed at a silver electrode. Chem. Phys. Lett. ***26***, 163–166.
2. Jeanmaire, D.L., and Van Duyne, R.P. (1977). Surface Raman spectroelectrochemistry: part I. Heterocyclic, aromatic, and aliphatic amines adsorbed on the anodized silver electrode. J. Electroanal. Chem. ***84***, 1–20.
3. Alessandri, I., and Lombardi, J.R. (2016). Enhanced Raman scattering with dielectrics. Chem. Rev. ***116***, 14921–14981.
4. Schlücker, S. (2014). Surface-enhanced Raman spectroscopy: concepts and chemical applications. Angew. Chem. Int. Ed. ***53***, 4756–4795.
5. Ding, S.Y., Yi, J., Li, J.-F., et al. (2016). Nanostructure-based plasmon-enhanced Raman spectroscopy for surface analysis of materials. Nat. Rev. Mater. ***1***, 16021–16037.
6. Le Ru, E.C., and Etchegoin, P.G. (2006). Rigorous justification of the $|E|^4$ enhancement factor in surface enhanced Raman spectroscopy. Chem. Phys. Lett. ***423***, 63–66.
7. Camden, J.P., Dieringer, J.A., Wang, Y., et al. (2008). Probing the structure of single-molecule surface-enhanced Raman scattering hot spots. J. Am. Chem. Soc. ***130***, 12616–12617.
8. Radziuk, D., and Moehwald, H. (2015). Prospects for plasmonic hot spots in single molecule SERS towards the chemical imaging of live cells. Phys. Chem. Chem. Phys. ***17***, 21072–21093.
9. Petryayeva, E., and Krull, U.J. (2011). Localized surface plasmon resonance: nanostructures, bioassays and biosensing-a review. Anal. Chim. Acta ***706***, 8–24.
10. Fang, Y., Seong, N.H., and Dlott, D.D. (2008). Measurement of the distribution of site enhancements in surface-enhanced Raman scattering. Science ***321***, 388–392.
11. Sun, Y., and Xia, Y. (2002). Shape-controlled synthesis of gold and silver nanoparticles. Science ***298***, 2176–2179.
12. Lee, P.C., and Meisel, D. (1982). Adsorption and surface-enhanced Raman of dyes on silver and gold sols. J. Phys. Chem. ***86***, 3391–3395.
13. Li, J.F., Zhang, Y.J., Ding, S.Y., et al. (2017). Core-shell nanoparticle-enhanced Raman spectroscopy. Chem. Rev. ***7***, 5002–5069.
14. Kim, A., Ou, F.S., Ohlberg, D.A., et al. (2011). Study of molecular trapping inside gold nanofinger arrays on surface-enhanced Raman substrates. J. Am. Chem. Soc. ***133***, 8234–8239.
15. Diebold, E.D., Peng, P., and Mazur, E. (2009). Isolating surface-enhanced Raman scattering hot spots using multiphoton lithography. J. Am. Chem. Soc. ***131***, 16356–16357.
16. Ward, D.R., Grady, N.K., Levin, C.S., et al. (2007). Electromigrated nanoscale gaps for surface-enhanced Raman spectroscopy. Nano Lett. ***7***, 1396–1400.
17. Lee, H.K., Lee, Y.H., Koh, C.S.L., et al. (2019). Designing surface-enhanced Raman scattering (SERS) platforms beyond hotspot engineering: emerging opportunities in analyte manipulations and hybrid materials. Chem. Soc. Rev. ***48***, 731–756.
18. Jensen, L., Aikens, C.M., and Schatz, G.C. (2008). Electronic structure methods for studying surface-enhanced Raman scattering. Chem. Soc. Rev. ***37***, 1061–1073.
19. Lombardi, J.R., and Birke, R.L. (2014). Theory of surface-enhanced Raman scattering in semiconductors. J. Phys. Chem. C ***118***, 11120–11130.
20. Lombardi, J.R., and Birke, R.L. (2009). A unified view of surface-enhanced Raman scattering. Acc. Chem. Res. ***42***, 734–742.
21. Zrimsek, A.B., Chiang, N., Mattei, M., et al. (2017). Single-molecule chemistry with surface- and tip-enhanced Raman spectroscopy. Chem. Rev. ***117***, 7583–7613.
22. Dong, B., Liu, L., Xu, H., et al. (2010). Experimental and theoretical evidence for the chemical mechanism in SERS of rhodamine 6G adsorbed on colloidal silver excited at 1064 nm. J. Raman Spectrosc. ***7***, 719–720.
23. Chenal, C., Birke, R.L., and Lombardi, J.R. (2008). Determination of the degree of charge-transfer contributions to surface-enhanced Raman spectroscopy. Chemphyschem ***9***, 1617–1623.
24. Lombardi, J.R., and Birke, R.L. (2008). A unified approach to surface-enhanced Raman spectroscopy. J. Phys. Chem. C ***112***, 5605–5617.
25. Moskovits, M. (1982). Surface selection rules. J. Chem. Phys. ***77***, 4408–4416.
26. Gao, X., Davies, J.P., and Weaver, M.J. (1990). A test of surface selection rules for surface-enhanced Raman scattering: the orientation of adsorbed benzene and monosubstituted benzenes on gold. J. Phys. Chem. ***94***, 6858–6864.
27. Langer, J., Jimenez de Aberasturi, D., Aizpurua, J., et al. (2020). Present and future of surface-enhanced Raman scattering. ACS Nano ***14***, 28–117.
28. Hu, W., Duan, S., Zhang, G., et al. (2015). Quasi-analytical approach for modeling of surface-enhanced Raman scattering. J. Phys. Chem. C ***119***, 28992–28998.
29. Xia, L., Chen, M., Zhao, X., et al. (2014). Visualized method of chemical enhancement mechanism on SERS and TERS. J. Raman Spectrosc. ***45***, 533–540.
30. An, P., Anumula, R., Wu, H., et al. (2018). Charge transfer interactions of pyrazine with Ag_{12} clusters towards precise SERS chemical mechanism. Nanoscale ***10***, 16787–16794.
31. Ling, X., Xie, L., Fang, Y., et al. (2010). Can graphene be used as a substrate for Raman enhancement. Nano Lett. ***10***, 553–561.
32. Xu, H., Xie, L., Zhang, H., et al. (2011). Effect of graphene Fermi level on the Raman scattering intensity of molecules on graphene. ACS Nano ***5***, 5338–5344.
33. Feng, S., Dos Santos, M.C., Carvalho, B.R., et al. (2016). Ultrasensitive molecular sensor using N-doped graphene through enhanced Raman scattering. Sci. Adv. ***2***, 1600322.
34. Yang, H., Hu, H., Ni, Z., et al. (2013). Comparison of surface-enhanced Raman scattering on graphene oxide, reduced graphene oxide and graphene surfaces. Carbon ***62***, 422–429.
35. Huh, S., Park, J., Kim, Y.S., et al. (2011). UV/ozone-oxidized large-scale graphene platform with large chemical enhancement in surface-enhanced Raman scattering. ACS Nano ***5***, 9799–9806.
36. Liu, D., Chen, X., Hu, Y., et al. (2018). Raman enhancement on ultra-clean graphene quantum dots produced by quasi-equilibrium plasma-enhanced chemical vapor deposition. Nat. Commun. ***9***, 193.
37. Das, R., Parveen, S., Bora, A., et al. (2020). Origin of high photoluminescence yield and high SERS sensitivity of nitrogen-doped graphene quantum dots. Carbon ***160***, 273–286.
38. Ling, X., Fang, W., Lee, Y.H., et al. (2014). Raman enhancement effect on two-dimensional layered materials: graphene, h-BN and MoS_2. Nano Lett. ***14***, 3033–3040.
39. Meng, L., Hu, S., Xu, C., et al. (2018). Surface enhanced Raman effect on CVD growth of WS_2 film. Chem. Phys. Lett. ***707***, 71–74.
40. Zheng, Z., Cong, S., Gong, W., et al. (2017). Semiconductor SERS enhancement enabled by oxygen incorporation. Nat. Commun. ***8***, 1993.
41. Muehlethaler, C., Considine, C.R., Menon, V., et al. (2016). Ultrahigh Raman enhancement on monolayer MoS_2. ACS Photon. ***3***, 1164–1169.
42. Liu, Y., Gao, Z., Chen, M., et al. (2018). Enhanced Raman scattering of CuPc films on imperfect WSe_2 monolayer correlated to exciton and charge-transfer resonances. Adv. Func. Mater. ***28***, 1805710.
43. Sun, L., Hu, H., Zhan, D., et al. (2014). Plasma modified MoS_2 nanoflakes for surface enhanced Raman scattering. Small ***10***, 1090–1095.
44. Yin, Y., Miao, P., Zhang, Y., et al. (2017). Significantly increased Raman enhancement on MoX_2 (X=S,Se) monolayers upon phase transition. Adv. Funct. Mater. ***27***, 1606694.
45. Tao, L., Chen, K., Chen, Z., et al. (2018). 1T′ transition metal telluride atomic layers for plasmon-free SERS at femtomolar levels. J. Am. Chem. Soc. ***140***, 8696–8704.
46. Song, X., Wang, Y., Zhao, F., et al. (2019). Plasmon-free surface-enhanced Raman spectroscopy using metallic 2D materials. ACS Nano ***13***, 8312–8319.
47. Liu, M., Shi, Y., Wu, M., et al. (2020). UV surface-enhanced Raman scattering properties of $SnSe_2$ nanoflakes. J. Raman Spectrosc. ***7***, 1–6.
48. Hou, X., Zhang, X., Ma, Q., et al. (2020). Alloy engineering in few-layer manganese phosphorus trichalcogenides for surface-enhanced Raman scattering. Adv. Funct. Mater. ***30***, 1910171.
49. Naguib, M., Kurtoglu, M., Presser, V., et al. (2011). Two-dimensional nanocrystals produced by exfoliation of Ti_3AlC_2. Adv. Mater. ***23***, 4248–4253.
50. Sarycheva, A., Makaryan, T., Maleski, K., et al. (2017). Two-dimensional titanium carbide (MXene) as surface-enhanced Raman scattering substrate. J. Phys. Chem. C ***121***, 19983–19988.
51. Li, G., Gong, W.B., Qiu, T., et al. (2020). Surface-modified two-dimensional titanium carbide sheets for intrinsic vibrational signal-retained surface-enhanced Raman scattering with ultrahigh uniformity. ACS Appl. Mater. Inter. ***12***, 23523–23531.
52. Ye, Y., Yi, W., Liu, W., et al. (2020). Remarkable surface-enhanced Raman scattering of highly crystalline monolayer Ti_3C_2 nanosheets. Sci. China Mater. ***63***, 794–805.
53. Limbu, T.B., Chitara, B., Orlando, J.D., et al. (2020). Green synthesis of reduced $Ti_3C_2T_x$ MXene nanosheets with enhanced conductivity, oxidation stability, and SERS activity. J. Mater. Chem. C ***8***, 4722–4731.
54. Soundiraraju, B., and George, B.K. (2017). Two-dimensional titanium nitride (Ti_2N) MXene: synthesis, characterization, and potential application as surface-enhanced Raman scattering substrate. ACS Nano ***11***, 8892–8900.
55. Yang, L., Jiang, X., Ruan, W., et al. (2008). Observation of enhanced Raman scattering for molecules adsorbed on TiO_2 nanoparticles: charge-transfer contribution. J. Phys. Chem. C ***112***, 20095–20098.
56. Musumeci, A., Gosztola, D., Schiller, T., et al. (2009). SERS of semiconducting nanoparticles (TiO_2 hybrid composites). J. Am. Chem. Soc. ***131***, 6040–6041.
57. Qi, D., Lu, L., Wang, L., et al. (2014). Improved SERS sensitivity on plasmon-free TiO_2 photonic microarray by enhancing light-matter coupling. J. Am. Chem. Soc. ***136***, 9886–9889.
58. Alessandri, I. (2013). Enhancing Raman scattering without plasmons: Unprecedented sensitivity achieved by TiO_2 shell-based resonators. J. Am. Chem. Soc. ***135***, 5541–5544.
59. Bontempi, N., Carletti, L., De Angelis, C., et al. (2016). Plasmon-free SERS detection of environmental CO_2 on TiO_2 surfaces. Nanoscale ***8***, 3226–3231.
60. Ji, W., Li, L., Song, W., et al. (2019). Enhanced Raman scattering by ZnO superstructures: synergistic effect of charge transfer and Mie resonances. Angew. Chem. ***58***, 14452–14456.

61. Yang, L., Gong, M., Jiang, X., et al. (2015). Investigation on SERS of different phase structure TiO_2 nanoparticles. J. Raman Spectrosc. ***46***, 287–292.
62. Yu, Y., Du, J., and Jing, C. (2019). Remarkable surface-enhanced Raman scattering on self-assembled {201} anatase. J. Mater. Chem. C ***7***, 14239–14244.
63. Wang, X., Shi, W., Jin, Z., et al. (2017). Remarkable SERS activity observed from amorphous ZnO nanocages. Angew. Chem. Int. Ed. ***56***, 9851–9855.
64. Wang, X., Shi, W., Wang, S., et al. (2019). Two-dimensional amorphous TiO_2 nanosheets enabling high-efficiency photoinduced charge transfer for excellent SERS activity. J. Am. Chem. Soc. ***141***, 5856–5862.
65. Dharmalingam, P., Venkatakrishnan, K., and Tan, B. (2019). An atomic-defect enhanced Raman scattering (DERS) quantum probe for molecular level detection—breaking the SERS barrier. Appl. Mater. Today ***16***, 28–41.
66. Cong, S., Geng, F., and Zhao, Z. (2016). Tungsten oxide materials for optoelectronic applications. Adv. Mater. ***28***, 10518–10528.
67. Cong, S., Yuan, Y., Chen, Z., et al. (2015). Noble metal-comparable SERS enhancement from semiconducting metal oxides by making oxygen vacancies. Nat. Commun. ***6***, 7800.
68. Fan, X., Li, M., Hao, Q., et al. (2019). High SERS sensitivity enabled by synergistically enhanced photoinduced charge transfer in amorphous nonstoichiometric semiconducting films. Adv. Mater. Inter. ***6***, 1901133.
69. Wu, H., Wang, H., and Li, G. (2017). Metal oxide semiconductor SERS-active substrates by defect engineering. Analyst ***142***, 326–335.
70. Cao, Y., Liang, P., Dong, Q., et al. (2019). Facile reduction method synthesis of defective MoO_{2-x} nanospheres used for SERS detection with high chemical enhancement. Anal. Chem. ***91***, 8683–8690.
71. Manthiram, K., and Alivisatos, A.P. (2012). Tunable localized surface plasmon resonances in tungsten oxide nanocrystals. J. Am. Chem. Soc. ***134***, 3995–3998.
72. Wang, J., Yang, Y., Li, H., et al. (2019). Stable and tunable plasmon resonance of molybdenum oxide nanosheets from the ultraviolet to the near-infrared region for ultrasensitive surface-enhanced Raman analysis. Chem. Sci. ***10***, 6330–6335.
73. Hou, X., Luo, X., Fan, X., Peng, Z., and Qiu, T. (2019). Plasmon-coupled charge transfer in WO_{3-x} semiconductor nanoarrays: toward highly uniform silver-comparable SERS platforms. Phys. Chem. Chem. Phys. ***21***, 2611–2618.
74. Zhang, Q., Li, X., Ma, Q., Zhang, Q., Bai, H., Yi, W., Liu, J., Han, J., and Xi, G. (2017). A metallic molybdenum dioxide with high stability for surface enhanced Raman spectroscopy. Nat. Commun. ***8***, 14903.
75. Ye, Y., Chen, C., Bai, H., et al. (2020). Quasi-metallic tungsten oxide nanodendrites with high stability for surface-enhanced Raman scattering. Cell Rep. Phys. Sci. ***1***, 10031–10049.
76. Cong, S., Wang, Z., Gong, W., et al. (2019). Electrochromic semiconductors as colorimetric SERS substrates with high reproducibility and renewability. Nat. Commun. ***10***, 678.
77. Zhou, C., Sun, L., Zhang, F., et al. (2019). Electrical tuning of the SERS enhancement by precise defect density control. ACS Appl. Mater. Inter. ***11***, 34091–34099.
78. Kudelski, A., Grochala, W., Janik-Czachor, M., et al. (1998). Surface-enhanced Raman scattering (SERS) at Copper(I) oxide. J. Raman Spectrosc. ***29***, 431–435.
79. Jiang, L., You, T., Yin, P., et al. (2013). Surface-enhanced Raman scattering spectra of adsorbates on Cu_2O nanospheres: charge-transfer and electromagnetic enhancement. Nanoscale ***5***, 2784–2789.
80. Li, X., Shang, Y., Lin, J., et al. (2018). Temperature-induced stacking to create Cu_2O concave sphere for light trapping capable of ultrasensitive single-particle surface-enhanced Raman scattering. Adv. Funct. Mater. ***28***, 1801868.
81. Lin, J., Shang, Y., Li, X., et al. (2017). Ultrasensitive SERS detection by defect engineering on single Cu_2O superstructure particle. Adv. Mater. ***29***, 1604797.
82. Shan, Y., Zheng, Z., Liu, J., et al. (2017). Niobium pentoxide: a promising surface-enhanced Raman scattering active semiconductor substrate. NPJ Comput. Mater. ***3***, 11–18.
83. Yang, L., Peng, Y., Yang, Y., et al. (2019). A novel ultra-sensitive semiconductor SERS substrate boosted by the coupled resonance effect. Adv. Sci. (Weinh) ***6***, 1900310.
84. Tian, Z., Bai, H., Chen, C., et al. (2019). Quasi-metal for highly sensitive and stable surface-enhanced Raman scattering. iScience ***19***, 836–849.
85. Sun, H., Cong, S., Zheng, Z., et al. (2018). Metal-organic frameworks as surface enhanced Raman scattering substrates with high tailorability. J. Am. Chem. Soc. ***141***, 870–878.
86. Su, X., Ma, H., Wang, H., et al. (2018). Surface-enhanced Raman scattering on organic-inorganic hybrid perovskites. Chem. Commun. (Camb) ***54***, 2134–2137.
87. Yilmaz, M., Ozdemir, M., Erdogan, H., et al. (2015). Micro-/nanostructured highly crystalline organic semiconductor films for surface-enhanced Raman spectroscopy applications. Adv. Funct. Mater. ***25***, 5669–5676.
88. Yilmaz, M., Babur, E., Ozdemir, M., et al. (2017). Nanostructured organic semiconductor films for molecular detection with surface-enhanced Raman spectroscopy. Nat. Mater. ***16***, 918–924.
89. Demirel, G., Gieseking, R.L.M., Ozdemir, R., et al. (2019). Molecular engineering of organic semiconductors enables noble metal-comparable SERS enhancement and sensitivity. Nat. Commun. ***10***, 5502–5511.
90. Tan, Y., Ma, L., Gao, Z., et al. (2017). Two-dimensional heterostructure as a platform for surface-enhanced Raman scattering. Nano Lett. ***17***, 2621–2626.
91. Ghopry, S.A., Alamri, M.A., Goul, R., et al. (2019). Extraordinary sensitivity of surface--enhanced Raman spectroscopy of molecules on MoS_2 (WS_2) nanodomes/graphene van der Waals heterostructure substrates. Adv. Opt. Mater. ***7***, 1801249.
92. Seo, J., Lee, J., Kim, Y., et al. (2020). Ultrasensitive plasmon-free surface-enhanced Raman spectroscopy with femtomolar detection limit from 2D van der Waals heterostructure. Nano Lett. ***20***, 1620–1630.
93. Li, M., Fan, X., Gao, Y., et al. (2019). $W_{18}O_{49}$/monolayer MoS_2 heterojunction-enhanced Raman scattering. J. Phys. Chem. Lett. ***10***, 4038–4044.
94. Hu, L., Amini, M.N., Wu, Y., et al. (2018). Charge transfer doping modulated Raman scattering and enhanced stability of black phosphorus quantum dots on a ZnO nanorod. Adv. Opt. Mater. ***6***, 1800440.
95. Dandu, M., Watanabe, K., Taniguchi, T., et al. (2020). Spectrally tunable, large Raman enhancement from nonradiative energy transfer in the van der Waals heterostructure. ACS Photon. ***7***, 519–527.
96. Fateixa, S., Nogueira, H.I., and Trindade, T. (2015). Hybrid nanostructures for SERS: materials development and chemical detection. Phys. Chem. Chem. Phys. ***17***, 21046–21071.
97. Xu, W., Ling, X., Xiao, J., et al. (2012). Surface enhanced Raman spectroscopy on a flat graphene surface. Proc. Natl. Acad. Sci. USA ***109***, 9281–9286.
98. Dutta, S., Ray, C., Sarkar, S., et al. (2013). Silver nanoparticle decorated reduced graphene oxide (rGO) nanosheet: a platform for SERS based low-level detection of uranyl ion. ACS Appl. Mater. Inter. ***5***, 8724–8732.
99. Qu, L., Wang, N., Xu, H., et al. (2017). Gold nanoparticles and g-C_3N_4-intercalated graphene oxide membrane for recyclable surface enhanced Raman scattering. Adv. Funct. Mater. ***27***, 1701714.
100. Yu, M., Liu, S., Su, D., et al. (2019). Controllable MXene nano-sheet/Au nanostructure architectures for the ultra-sensitive molecule Raman detection. Nanoscale ***11***, 22230–22236.
101. Zhou, J., Zhang, J., Yang, H., et al. (2019). Plasmon-induced hot electron transfer in Au-ZnO heterogeneous nanorods for enhanced SERS. Nanoscale ***11***, 11782–11788.
102. O'Neill, D.B., Prezgot, D., Ianoul, A., et al. (2020). Silver nanocubes coated in ceria: core/shell size effects on light-induced charge transfer. ACS Appl. Mater. Inter. ***12***, 1905–1912.
103. Gu, L.J., Ma, C.L., Zhang, X.H., et al. (2018). Populating surface-trapped electrons towards SERS enhancement of $W_{18}O_{49}$ nanowires. Chem. Commun. (Camb) ***54***, 6332–6335.
104. Wang, Y., Liu, J., Ozaki, Y., et al. (2019). Effect of TiO_2 on altering direction of interfacial charge transfer in a TiO_2-Ag-MPY-FePc system by SERS. Angew. Chem. Int. Ed. ***24***, 8172–8176.
105. Ben-Jaber, S., Peveler, W.J., Quesada-Cabrera, R., et al. (2016). Photo-induced enhanced Raman spectroscopy for universal ultra-trace detection of explosives, pollutants and biomolecules. Nat. Commun. ***7***, 12189.
106. Al-Shammari, R.M., Baghban, M.A., Al-Attar, N., et al. (2018). Photoinduced enhanced Raman from lithium niobate on insulator template. ACS Appl. Mater. Inter. ***10***, 30871–30878.
107. Zhou, L., Zhou, J., Lai, W., Yang, X., et al. (2020). Irreversible accumulated SERS behavior of the molecule-linked silver and silver-doped titanium dioxide hybrid system. Nat. Commun. ***11***, 1785.
108. Sidorov, A., Vashkinskaya, O., Grigorieva, A., et al. (2014). Entrapment into charge transfer complexes for resonant Raman scattering enhancement. Chem. Commun. (Camb) ***50***, 6468–6470.
109. Wang, Y., Ji, W., Sui, H., et al. (2014). Exploring the effect of intermolecular H-bonding: a study on charge-transfer contribution to surface-enhanced Raman scattering of p-mercaptobenzoic acid. J. Phys. Chem. C ***118***, 10191–10197.
110. Li, H., Dai, H., Zhang, Y., et al. (2017). Surface-enhanced Raman spectra promoted by a finger press in an all-solid-state flexible energy conversion and storage film. Angew. Chem. Int. Ed. Engl. ***56***, 2649–2654.
111. Ji, W., Kitahama, Y., Han, X., et al. (2012). pH-dependent SERS by semiconductor-controlled charge-transfer contribution. J. Phys. Chem. C ***116***, 24829–24836.
112. Sun, H., Yao, M., Song, Y., et al. (2019). Pressure-induced SERS enhancement in a MoS_2/Au/R6G system by a two-step charge transfer process. Nanoscale ***11***, 21493–21501.
113. He, S., Liu, X., Zhang, W., et al. (2015). Discrimination of the *Coptis chinensis* geographic origins with surface enhanced Raman scattering spectroscopy. Chemometrics Intell. Lab. Syst. ***146***, 472–477.
114. He, S., Xie, W., Zhang, W., et al. (2015). Multivariate qualitative analysis of banned additives in food safety using surface enhanced Raman scattering spectroscopy. Spectrochim Acta A. Mol. Biomol. Spectrosc. ***137***, 1092–1099.
115. Xie, W., He, S., Xia, L., et al. (2015). Fabrication of a trans-scale bimetallic synergistic enhanced Raman scattering substrate with high surface-enhanced Raman scattering activity. Anal. Methods ***7***, 1676–1679.
116. Jing, X., Chang, L., Shi, L., et al. (2020). Au film-Au@Ag core-shell nanoparticle structured surface-enhanced Raman spectroscopy aptasensor for accurate ochratoxin A detection. ACS Appl. Bio Mater. ***3***, 2385–2391.

117. Zhao, Y., Zheng, F., Ke, W., et al. (2019). Gap-tethered Au@AgAu Raman tags for the ratiometric detection of MC-LR. Anal. Chem. ***91***, 7162–7172.
118. Qiao, X., Su, B., Liu, C., et al. (2018). Selective surface enhanced Raman scattering for quantitative detection of lung cancer biomarkers in superparticle@MOF structure. Adv. Mater. ***30***, 1702275.
119. Ganesh, S., Venkatakrishnan, K., and Tan, B. (2020). Quantum scale organic semiconductors for SERS detection of DNA methylation and gene expression. Nat. Commun. ***11***, 1135.
120. Haldavnekar, R., Venkatakrishnan, K., and Tan, B. (2018). Non plasmonic semiconductor quantum SERS probe as a pathway for in vitro cancer detection. Nat. Commun. ***9***, 3065.
121. Lin, J., Ren, W., Li, A., et al. (2020). Crystal-amorphous core-shell structure synergistically enabling TiO_2 nanoparticles' remarkable SERS sensitivity for cancer cell imaging. ACS Appl. Mater. Inter. ***12***, 4204–4211.
122. Wang, Y., Yu, Z., Han, X., et al. (2016). Charge-transfer-induced enantiomer selective discrimination of chiral alcohols by SERS. J. Phys. Chem. C ***120***, 29374–29381.
123. Wang, Y., Liu, J., Zhao, X., et al. (2019). A chiral signal-amplified sensor for enantioselective discrimination of amino acids based on charge transfer-induced SERS. Chem. Commun. (Camb) ***55***, 9697–9700.
124. de Nijs, B., Benz, F., Barrow, S.J., et al. (2017). Plasmonic tunnel junctions for single-molecule redox chemistry. Nat. Commun. ***8***, 994.
125. Zhan, C., Chen, X.J., Huang, Y.F., et al. (2019). Plasmon-mediated chemical reactions on nanostructures unveiled by surface-enhanced Raman spectroscopy. Acc. Chem. Res. ***52***, 2784–2792.
126. Dong, J.-C., Zhang, X.-G., Briega-Martos, V., et al. (2018). In situ Raman spectroscopic evidence for oxygen reduction reaction intermediates at platinum single-crystal surfaces. Nat. Energy ***4***, 60–67.
127. Du, L., Shi, G., Zhao, Y., et al. (2019). Plasmon-promoted electrocatalytic water splitting on metal-semiconductor nanocomposites: the interfacial charge transfer and the real catalytic sites. Chem. Sci. ***10***, 9605–9612.
128. Wang, X., Wang, Y., Sui, H., et al. (2016). Investigation of charge transfer in Ag/N719/TiO_2 interface by surface-enhanced Raman spectroscopy. J. Phys. Chem. C ***120***, 13078–13086.
129. Wang, X., Han, X.X., Ma, H., et al. (2018). Reduced charge-transfer threshold in dye-sensitized solar cells with an Au@Ag/N3/n-TiO_2 structure as revealed by surface-enhanced Raman scattering. J. Phys. Chem. C ***122***, 12748–12760.
130. Ioffe, Z., Shamai, T., Ophir, A., et al. (2008). Detection of heating in current-carrying molecular junctions by Raman scattering. Nat. Nanotechnol ***3***, 727–732.
131. Zhang, H., Wei, J., Zhang, X.-G., et al. (2020). Plasmon-induced interfacial hot-electron transfer directly probed by Raman spectroscopy. Chem ***6***, 689–702.
132. Yang, G., Ivanov, I.N., Ruther, R.E., et al. (2018). Electrolyte solvation structure at solid-liquid interface probed by nanogap surface-enhanced Raman spectroscopy. ACS Nano ***12***, 10159–10170.
133. Glass, D., Cortés, E., Ben-Jaber, S., et al. (2019). Dynamics of photo-induced surface oxygen vacancies in metal-oxide semiconductors studied under ambient conditions. Adv. Sci. (Weinh) ***6***, 1901841.

ACKNOWLEDGMENTS

This work was supported by the National Natural Science Foundation of China (51772319, 51772320, 51972331, and 61575196), the Youth Innovation Promotion Association of the Chinese Academy of Sciences (2018356), the External Cooperation Program of the Chinese Academy of Sciences (121E32KYSB20190008), the Outstanding Youth Fund of Jiangxi Province (20192BCBL23027), the Natural Science Foundation of Jiangxi Province (20181ACB20011), the Six Talent Peaks Project of Jiangsu Province (XCL-170), the Science and Technology Project of Nanchang (2017-SJSYS-008), the Chongqing Talents Program (grant no. CQYC201905041), the Chongqing Scientific and Technological Program Project of China (cstc2019jcyj-msxmX0663), and the Science and Technology Research Program of Chongqing Municipal Education Commission (grant no.KJQN201904102).

DECLARATION OF INTERESTS

The authors declare no competing interests.

LEAD CONTACT WEBSITE

http://orcid.org/0000-0002-9756-9994; http://orcid.org/0000-0002-9327-9893.